

Copyright

By

China-EU Institute for Clean And Renewable Energy

2013

**The Thesis committee for China- EU Institute for Clean And Renewable Energy
Certifies that this is the approved version of the following thesis:**

**Design and optimization of turbine system for megawatt
level parabolic trough solar thermal power station**

**APPROVED BY
JURY COMMITTEE:**

Chairperson: _____

(Name typed on line, omitting Ph.D. or Dr.)

Committee Member: _____

(Name typed on line, omitting Ph.D. or Dr.)

Committee Member: _____

(Name typed on line, omitting Ph.D. or Dr.)

(No page number on the actual copyright page, page number: bottom right 8)

**ICARE**

中欧清洁与可再生能源学院

China-EU Institute for Clean and Renewable Energy

华中科技大学 Huazhong University of Science & Technology

**Design and optimization of turbine system for megawatt
level parabolic trough solar thermal power station**

Full Name of Student: LI Yueqin

Chinese supervisor: Huang Shuhong

European co-supervisor/reader: Quentin Falcoz

Submission Date: 2013.9.18.

Abstract

Electricity generation from solar thermal energy can be a useful alternative concerning fossil fuel conservation as well as CO₂ emission reduction. In China, ever since 2005, near 10 demonstration CSP projects have been set up, among which nearly half are using parabolic trough technology. The subject of this research stems from one of the demonstration project proposals which concerns building a 1MW parabolic trough solar power plant near Liangzi Lake, Wuhan.

In this thesis, a typical process of one dimensional steam turbine flow path design was analyzed first, then an optimized design method was proposed. The new design process was realized in Borland Delphi based on object oriented programming paradigm and MVC software architecture pattern, forming a practical and user friendly design software named ‘STFPD (Steam Turbine Flow Path Design)’, the results were compared with design data from an existing 25MW condensing steam turbine. Furthermore, several cases were studied and compared regarding the design schemes of power block for 1MW Liangzi Lake parabolic trough solar thermal power plant by STFPD. Thereby a conclusion of features for megawatt level solar thermal specialized steam turbines was drawn.

Keywords: PT solar thermal, turbine flow path design, optimization, software platform

Table of Contents

Abstract	4
Table of Contents	v
List of Figures	viii
List of Tables	ix
Notation	x
Acronyms and Abbreviations.....	xii
Chapter 1 Introduction	1
1.1 Background	1
1.2 Literature Review	1
1.2.1 Power blocks of parabolic trough solar thermal power plant..	1
1.2.2 Steam turbine flow path design.....	3
1.2.3 Turbine flow path design softwares	6
1.3 Thesis Objectives	8
1.4 Thesis Outline.....	8
Chapter 2 Basic Theories for turbine system design	9
2.1 Fundamentals of Rankine Cycle	9
2.2 Basic theories for one dimensional turbine flow path design	12
2.2.1 The one dimensional flow theory.....	13
2.2.2 Extra Loss models	17
Chapter 3 Optimization	19
3.1 Objectives.....	19
3.2 Optimization Model	19
3.3 Methodology	20

3.3.1	Coupling based on (fixed) post stage points	20
3.3.2	Coupling based on (fixed) extraction points	22
3.3.3	Coupling based on both extraction points and post stage points	23
3.4	Tests and conclusions	24
3.4.1	Case Settings	24
3.4.2	Results and comparisons	26
3.4.3	Conclusions	27
Chapter 4	Establishment of STFPD (Steam Turbine Flow Path Design) software platform	28
4.1	Methodology	28
4.1.1	Requirements analysis.....	28
4.1.2	Programming paradigms	29
4.2	General description of STFPD	30
4.2.1	General introduction.....	30
4.2.2	Module Introduction.....	33
4.3	Data structure	40
4.4	Program Test.....	49
Chapter 5	Design of turbine system for a 1MW parabolic trough solar thermal power plant using STFPD	52
5.1	Case description	52
5.2	Case studies	54
5.3	Conclusions	55
Chapter 6	Conclusions and future work.....	57
6.1	Research conclusions	57
6.2	Future work and suggestions.....	57

Acknowledgements	59
References	60

List of Figures

Figure 1.	The quasi-3D aerodynamic design process	3
Figure 2.	Simplified schematic diagram of the power block for the 5-MWe DSG solar power plant	6
Figure 3.	Super heat Rankine Cycle.....	9
Figure 4.	Regenerative Rankine Cycle	10
Figure 5.	Mathematical model of heat regenerative system for 25MW power plant	10
Figure 6.	Rankine Cycle with reheat.....	12
Figure 7.	Relationship between ψ and Ω_m	15
Figure 8.	Calculation process for a dual row governing stage.....	17
Figure 9.	Optimization algorithm	20
Figure 10.	Coupling based on fixed post stage points	21
Figure 11.	Illustration of coupling based on fixed post stage points	21
Figure 12.	Coupling based on extraction points	22
Figure 13.	Coupling based on both sides of points	23
Figure 14.	Algorithm of the optimization process	24
Figure 15.	Initial settings	25
Figure 16.	Final curve of case 1	27
Figure 17.	Scope of work.....	29
Figure 18.	STFPD: Turbine Type Settings.....	31
Figure 19.	STFPD: Main Work Space	31
Figure 20.	STFPD: Progressive Design in the first round	32
Figure 21.	Algorithm of iteration.....	33
Figure 22.	Main Params (analysis) module	34
Figure 23.	h-s Chart	34
Figure 24.	Module 'Governing Stage'	35
Figure 25.	Module 'HRSys'.....	35
Figure 26.	'StageDivRef' sub-module	37
Figure 27.	'StageDiv' Module.....	37
Figure 28.	Module 'Coupling'	38
Figure 29.	Module 'Stage Calculation'	39
Figure 30.	Sub Module showing stage by stage calculation results.....	39
Figure 31.	Module 'Section Calculation'	40
Figure 32.	Illustration of the MVC architecture pattern	41
Figure 33.	Architecture of STFPD	41
Figure 34.	Illustration of module structures.....	44
Figure 35.	Scheme of Liangzi Lake 1MW parabolic trough solar thermal power plant	52

List of Tables

Table 1. Information of power blocks of world's PT power plants using Steam Rankine Cycle ^[1-2]	2
Table 2. Technical data of SST-100	5
Table 3. Power block parameters for the 5-Mwe DSG solar power plant.....	6
Table 4. Design Point parameters in this case	24
Table 5. Operations for each case	25
Table 6. Case 1_Stage enthalpy drop distribution and its final indexes	26
Table 7. Case 2_Stage enthalpy drop distribution and its final indexes	26
Table 8. List of basic units.....	42
Table 9. Structure analysis of STFPD.....	45
Table 10. Comparison between benchmark and STFPD results (Governing Stage).....	49
Table 11. Comparison between Bench Mark and STFPD results (pressure stage #1)	50
Table 12. A plan for solar field using ET150 parabolic trough collector	52
Table 13. Design Point parameters for the 1MWe Rankine power cycle.....	53
Table 14. Case comparisons	54

Notation

$\Delta D_e[i]$	extraction steam flow rate for heater i
$h_e[i]$	extraction steam enthalpy for heater i
$h'_e[i]$	drain enthalpy for heater i
$h_{w1}[i]$	inlet feed water enthalpy for heater i
$h_{w2}[i]$	outlet feed water enthalpy for heater i
D_{fw}	mass flow rate of feed water
η_h	thermal efficiency of heater i
D_{cw}	mass flow rate of condensing water
ΔD_g	mass flow rate of extraction steam at deaerator
G	Mass flow rate
n	Rotational speed
d_m	Mean diameter of stage
Eh_t	Enthalpy distribution of stage
x_a	Velocity ratio of stage
Ω_m	Degree of reaction
Δh_n	Enthalpy drop in nozzle
ε_n	steam flow state at the outlet of nozzle
C_1	nozzle outlet velocity
A_n	nozzle's outlet cross sectional area
μ_n	nozzle flow rate coefficient
l_n	Nozzle outlet height
e	Partial-arc admission degree
Δh_n	Nozzle loss
Δh_{w1}	stagnation parameters
Δh_b	Enthalpy drop in the rotor blade
Δh_b^*	stagnation enthalpy drop
w_{2t}	rotor blade outlet relative velocity
ψ	rotor blade velocity coefficient
$\Delta h_{b\xi}$	Rotor blade loss
A_b	rotor blade exit area
l_b^i	Rotor blade exit height
α_1	Inlet flow angle
α_2	outlet flow angle

β_2	relative outlet velocity angle
c_2	rotor blade absolute outlet velocity
Δh_{c2}	Carryover loss
Δh_u	Wheel periphery enthalpy drop
η_u	Efficiency of the wheel periphery
W_u	Wheel periphery power produced by 1 kg steam
η_w	Efficiency of the wheel periphery
Δh_l	Losses related to blade height
Δh_f	Friction and ventilation losses
Δh_p	Baffle leakage losses
Δh_{pt}	Blade tip losses
Δh_e	Losses due to partial-arc admission
Δh_x	Humidity losses
η_i	Stage efficiency
l	blade height
$\Delta h_u'$	rim enthalpy drop
d_b	mean line diameter of rotor blade
u	rim velocity
G	mass flow rate of the stage
v	specific volume of stage outlet point
δ_p	size of diaphragm air gap
d_p	diameter of diaphragm
z_p	the tooth number of shaft seal
δ_m	average axial air gap size of blade tip
α_1	the steam inlet direction angle
E_0	ideal energy of the stage
e	partial-arc admission degree
Z_m	nozzle set number
x_1, x_2	dryness fraction of stage inlet and outlet point
P_i	internal power
C_a	ideal nozzle outlet velocity
η_{ri}	turbine relative internal efficiency
η_i	turbine absolute internal efficiency

Acronyms and Abbreviations

PT	Parabolic trough
CSP	Concentrating solar power
SRC	Steam Rankine Cycle
STFPD	Steam turbine flow path design
MVC	Modeler-Viewer-Controller
GUI	Graphic User Interface

Chapter 1 Introduction

1.1 Background

Electricity generation from solar thermal energy can be a useful alternative concerning fossil fuel conservation as well as CO₂ emission reduction. Spain, U.S., Germany and Israel are the leading countries in this realm. Among various types of existing CSP plants, parabolic trough technology is mostly used. SolarPACE^[1] has done a brilliant job by compiling data on CSP projects around the world. The database includes plants that are either operational, under construction, or under development. According to it, 83 new parabolic trough projects are in record, compared to 10 in Linear Fresnel Reflector, 20 in power tower, and 2 in Dish/Engine.

The solar thermal electricity generation technology is still in the demonstration phase in China. Back to the 1970s, the CAS (Chinese Academy of Science) has done preliminary researches on PT technology. Then it was not until the year 2004 that the heat wave in R&D of CSP technology was introduced domestically. Ever since 2005, near 10 demonstration CSP projects have been set up, among which nearly half are using parabolic trough technology. The subject of this research stems from one of the demonstration project proposals concerning building a 1MW parabolic trough solar power plant near Liangzi River, Wuhan.

1.2 Literature Review

1.2.1 Power blocks of parabolic trough solar thermal power plant

General situation of power blocks in several power plants utilizing parabolic trough technology is displayed in Table.1. Based on collected data, turbine efficiency broadly ranges from 20% to 39%. It is obvious that the efficiency of turbine is closely related to solar field outlet temperature and its capacity. To be more specific, the higher the outlet temperature and the larger the size of the plant, the higher the turbine's efficiency. This trend is in accordance with the Rankine cycle theory.

Table 1. Information of power blocks of world's PT power plants using Steam Rankine Cycle^[1-2]

Project	Country	Com pleted	Capacit y /MW	η_{el} /%	Power cycle pressure /Mpa	Manufactuer	Solar resource kWh/m2/yr	LA/AA /m2	solar field inlet t /°C	solar field outlet t /°C	storage capacity /h
SEGS I	U.S.	1985	13.8	31.5	4	MHI	2725	82960(AA)		307	3
SEGS II	U.S.	1986	30	29.4	4	MHI	2725	190338(AA)		316	
SEGS III&IV	U.S.	1987	30	30.6	4	MHI	2725	230300(AA)		349	
SEGS V	U.S.	1988	30	30.6	4	MHI	2725	250500(AA)		349	
SEGS VI	U.S.	1989	30	37.5	4	MHI	2725	188000(AA)		390	
SEGS VII	U.S.	1989	30	37.5	4	MHI	2725	194280(AA)		390	
SEGS VIII	U.S.	1990	30	37.6	4	MHI	2725	464340(AA)		390	
SEGS IX	U.S.	1991	30	37.6	4	MHI	2725	483960(AA)		390	
Saguaro Power Plant	U.S.	2006	Net 1.0 Gross 1.2	20.7	2.23	Ormat (Israel)	2636	100000(AA)	120	300	non
Andasol 1	Spain	2008	Net 49.9 Gross 50	38.1	10	Siemens	2136	510120(AA)	293	393	7.5
Holaniku at Keahole Point	U.S.	2009	2					4047(LA)	93	176	2
Archimede	Italy	2010	Net 4.72 Gross 5	39.3	9.383	Tosi	1936	31860(AA)	290	550	8
Termesol 50	Spain	2011	49.9	38.1	10		2097	510120(AA)	293	393	7.5
Thai Solar Energy 1	Thailand	2012	5		3	MAN (MARC 2)		45000(AA)	201	340	non

A number of studies are dedicated to the performance of steam Rankine cycles integrated with PT technology. Niknia et al.^[3] carried out a simulation to examine the performance of a PT power plant integrated with an auxiliary boiler, they discussed the advantages of their system as compared to a fossil fuel based system. Montes et al.^[4] studied the effect of changing the solar multiple on the performance of PT combined with SRC. Zarza et al.^[5] presented the conceptual design of a solar power plant using direct steam generation in a PT field. Meanwhile, Wang et al.^[6] studied a regenerative organic Rankine cycle to utilize the solar energy over a low temperature range using flat plate solar collectors. Their study illustrated that increasing turbine inlet pressure and temperature or lowering the turbine back pressure could improve system performance. Fahad A. Al-Sulaiman^[7] investigated into the PT solar field sizing and

overall performance of different vapor cycles (including a binary vapor cycle and a steam Rankine cycle) in 2013. This study reveals that significant reduction in the solar field size is could be achieved due to the performance improvement by considering the binary vapor cycle as compared to a steam Rankine cycle with atmospheric condensing pressure; however, SRC with vacuum pressure presents the best performance and smallest solarfield size.

1.2.2 Steam turbine flow path design

The modern manifestation of a steam turbine was invented in 1884^[2] and the first commercialized steam turbine dates back to the year of 1897^[8]. Within more than a century's development, the technique is now mature with well-known theoretical foundations as well as abundant empirical facts. In recent decades, with the prosperity of computer science, this process relies more and more on computers.

At present, a standard steam turbine flow path designing process is composed of three major phases, namely the 1D design (preliminary design), 2D (Through flow design) design and 3D design (Airfoil design). Among these phases, 1D design focuses on the thermal dynamic design and initial shaping of flow path, 2D focuses on refined flow path shaping and 3D focuses on numerical simulation. The whole process is usually referred to as the quasi-3D aerodynamic design. Fig.1 is used to illustrate the modern design process:

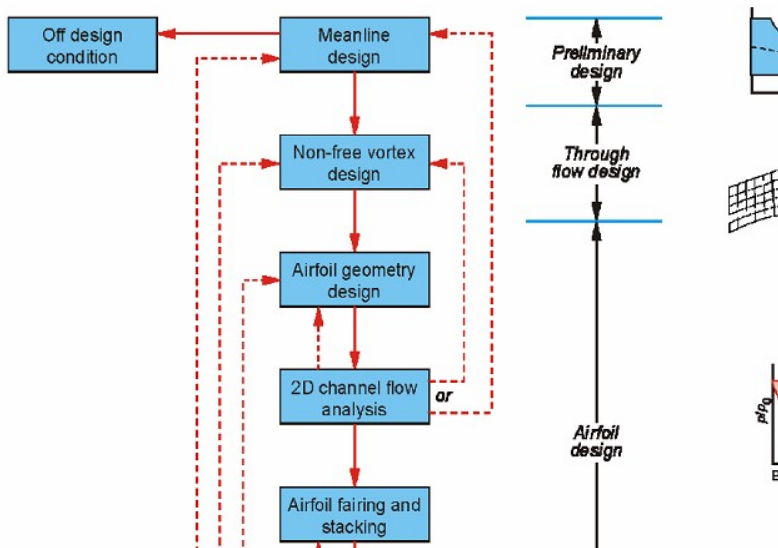


Figure 1. The quasi-3D aerodynamic design process

1D design is the oldest thus the most mature design method. It was not until 1950s that 2D design theory began to rise and further developed ever since^[9]. Using 1D design alone it is possible to get a basic steam turbine scheme, yet in the modern design process with the appliance of 2D and 3D design method it is possible to refine and optimize the scheme. This paper mainly focuses on the 1D design method.

The one dimensional design of a steam turbine is a well-known process with several separately outlined elementary theories. In general the major procedures include^[10]:

- 1) Initial data analysis : estimation of inlet steam flow rate D_0 , acquire approximate thermal dynamic process curve;
- 2) Turbine type settings;
- 3) Governing stage design (if necessary);
- 4) Heat regenerative system design and analysis;
- 5) Stage division and detailed calculation;

In general the one dimensional design of steam turbine proves to be a complicated process with numerous interactive design parameters, despite the fact that it is so theoretically simplified that it relies heavily on semi-experimental data and functions to avoid the complexity brought by advanced fluid mechanics. In one dimensional design, the key to finding a proper solution lies in the choice of independent and dependent variables as well as reasonable control of degree of freedom. If a heat regenerative system is included, it is essential to make sure the extraction point coincide with stage intervals. Most of the time revisions and iterations have to be carried out to meet this constraint.

There are various literatures focusing on steam turbine designing and its optimization. From 1980s on Chen Lingen did several reviews and published a series of papers focusing on optimization of both single stage and sections (stage groups). The methods include multiobjective optimum design and the genetic algorithm^[11-15]. Multiobjective optimum design method includes setting objectives, establishing constraints and using penalty function method to search for optimum results. The genetic algorithm is achieved by taking the maximum efficiency of the stage as the objective, along with a series of functions as constraints, the genetic algorithm process is later carried out to obtain optimal geometric and aerodynamic parameters. In commercial software Axstream, optimization is carried out in the way of generating the sets of input parameters for inverse problem solver with subsequent filtering the solutions obtained and selecting the best case. To guarantee the search move towards maximum of efficiency, when a best solution is found, the ranges not flagged as ‘manual’ are changed for +/-20% of corresponding parameter value at the best point^[16].

Worldwide well-known steam turbine manufacturers include Siemens, GE, Alstom, SKODA, KKK, Mitsubishi, TOSHIBA, domestic manufacturers include Harbin turbine co., Dongfang turbine co., Shanghai turbine co., Hangzhou turbine co., Nanjing turbine co., Qingdao turbine co. etc. Among them Siemens is pioneering commercial solutions in the CSP realm.

The SST series of Siemens, used by most Spanish and American solar thermal power plants prove to be a huge success with innovative design and high efficiency. The features of SST include^[17]:

- Cost effective, highly reliable solution;
- Fast and early layout planning;
- Short delivery times because of highly predefined design of both turboset and package;
- Short on-site erection: turbine skid and gearbox / oil unit fully assembled in the workshop before shipping to site;
- Compact design - oil system fully integrated into the base frame;
- Proven components: highly standardized, robust blading; reduction gears taken from the existing range of world-class gear manufacturers;
- Increased safety: no leaks towards hot pipes; oil and steam piping separated;
- Easy maintenance with low maintenance costs;

SST-100 is a type of turbine specially designed for capacity below 8.5MWe. As a single body turbine, SST-100 is designed for high thermo flexibility, permitting short start-up times and rapid load changes. Other features include single-casing multi-stage, highly predefined proven and compact design, workshop assembly, oil system integrated in base frame, separation of oil and steam piping. The technical data is shown in table 2.

Table 2. Technical data of SST-100^[18]

Power output	up to 8.5 MW
Rotational speed	up to 7,500 rpm
Inlet steam pressure	up to 65 bar / 945 psi
Inlet steam temperature	480 °C / 895 °F
Exhaust pressure	Back pressure: up to 10 bar (a) / 145 psi; Condensing: up to 1 bar / 14.5 psi
Exhaust area	0.22 m ² / 2.4 sq.ft.

In its back pressure application, SST-100 has up to six impulse stages. The rotor is made of solid forging or with forged discs shrink-mounted on the turbine shaft and keyed. It is short and rigid, resulting in operation well below first critical speed, using babbitt-lined sliding type bearings to assure a smooth and well-damped operation. The condensing form design is derived from the back pressure version and has up to seven impulse stages, including condensing stages, the exhaust casing is oriented downwards through the base frame or upwards, depending on the application. It also involves diaphragm carrier for the last three stages.

In defining specific features of a solar power steam turbine, a good example to learn from is the INDITEP^[19]. Project INIDITEP is a 5MWe parabolic trough solar power plant using DSG technology. In order to assure durability and reliability, the steam turbine included in the power block is KKK non-reheat superheated steam turbine

offered by PASCH (model CFR5G6a + AFA66GT5a).

Table 3. Power block parameters for the 5-Mwe DSG solar power plant

Manufacturer	KKK
Gross power(kWe)	5472
Net power(kWe)	5175
Net heat rate(kJ/kWh)	14,460
Gross efficiency(%)	26.34
Net efficiency(%)	24.9

The outlet of the turbine high-pressure stage is connected to the inlet of the low-pressure stage. The isentropic efficiency of the turbine is 72% at the nominal steam flow rate of 26 ton/h and decreases to 28% at 6 ton/h. One of the main advantages of this KKK turbo-generator is that with adequate inlet pipe purging, it can be started up directly without preheating, and is able to go from idle to rated conditions in a matter of minutes, which is a valuable characteristic for the operation of a power block fed by a solar field that has to be started up and shut-down daily.

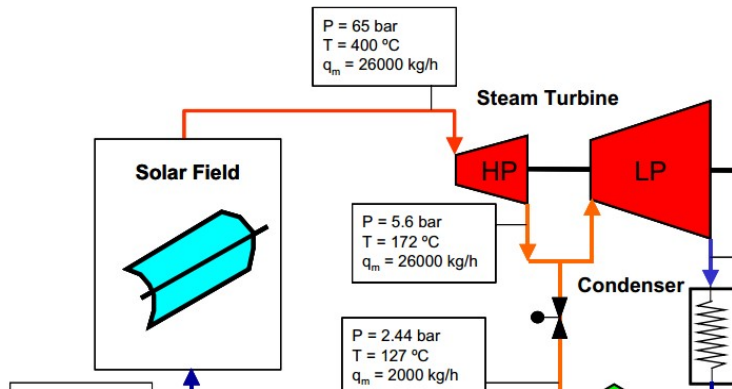


Figure 2. Simplified schematic diagram of the power block for the 5-MWe DSG solar power plant

1.2.3 Turbine flow path design softwares

A rich variety of simplified axial turbine design software has been developed thanks to the prosperity of computer science. However in view of the number of certain reasons these introducing to a design organization practice are highly difficult. Since the problem solution is in particularized software packages for turbomachines flowpaths conceptual design creation^[20]. For one thing different users may expect different types of steam turbines, which would result in differences in mathematical models, for the other on the availability of centralized information storage, uniform interface for control of the design process, inputting and mapping data, optimization subsystem etc, it is extremely complicated to decide a uniform framework and meet all the specific user requirements. In this paper, three different software approaches coming from three

different backgrounds have been studied individually.

1) Source Code attached to ‘Steam Turbine Course Design’^[21].

The source code attached to ‘Steam Turbine Course Design’ is divided into two major parts, namely the water and steam water property subprogram and the steam turbine thermal dynamic calculation subprogram. The latter subprogram is composed of 21 subroutines covering initial parameters’ setting and analysis, heat regenerative system design and analysis, stage distribution, stage by stage calculation and rebuild of steam water parameters, it also includes two varying working condition calculation subroutines using backward and sequence calculation method respectively. In addition, This program is suitable for designing steam turbines both with and without reheat system. But since the stage calculation is simplified to only consider subcritical situations, the software is not able to cope with designs concerning Laval nozzles.

In general this version of software is neatly designed with clear sequences and generates sound results. Developed by Matlab, it endows with typical features of a process oriented program. Due to the lack of GUI, users have to filter and analysis the data generated in each phase by themselves and feed them into the next step manually.

2) AxSTREAM^[16]

AxSTREAM is one of the most celebrated commercial software in the realm of turbine design. Its suite of multidisciplinary design, analysis and optimization software provides an integrated and streamlined solution that encompasses the complete process of conceptual flow path design for both radial and axial turbomachinery (turbines, compressors, fans, blowers, turbopumps etc).

In the preliminary design phase of AxSTREAM, users need to decide a wide range of capabilities to rapidly select optimal main flow path parameters, such as the number of stages, geometrical dimensions and angles, heat drop distributions and so on. This process requires reviewing a great number of alternative designs to select a most effective solution point, i.e. the best design for a certain quality/constraints criterion. Also the preliminary design procedure is powered with inverse task that uses a handful of design and operational parameters to generate flow path geometry.

Principal parameters to be defined during design phase are: Basic meridional dimensions (diameters, blade heights), blades aerodynamic geometry (angles distribution, twist, lean) and basic axial dimensions, clearances. Then the solution generator automatically generates a set of solutions for given specifications. After that users are guided to define most promising solutions with Preliminary Design Space Explorer.

3) Master thesis ‘R&D on a software for thermodynamic designing of industrial steam turbines’ from Li Wei, Zhe Jiang University^[22].

In his work Li Wei used the ideas of modularization design and product seriation,

accompanied with scientific methods obtained from software engineering. The software is specialized for industrial steam turbines (under 100MW) with a limitation of steam extraction number of two. Available industrial turbine types include condensing steam turbine and backpressure steam turbine. Apart from basic procedures, it also includes varying working condition calculation. The software was developed under the environment of Microsoft VC++6.0.

1.3 Thesis Objectives

- 1) To study the common design method of turbine and come up with a new optimization method.
- 2) To establish a software platform, realizing the basic functions of the steam turbine system design and its optimization.
- 3) To design the turbine system of a 1MW parabolic trough solar thermal power plant.

1.4 Thesis Outline

This thesis is organized in the following order:

Chapter 2 analyses in detail the method of thermal dynamic design for Rankine Cycle.

Chapter 3 introduces a new optimize method concerning the one dimensional thermal dynamic design process.

Chapter 4 describes the framework of the software, followed by detailed module introduction and data structure description. The software is then tested on a benchmark.

Chapter 5 presents the steam turbine design software integrated with solar thermal. Among various tests, three cases were picked out and compared to bring out the solutions for a certain PTC power plant.

Chapter 6 gives the conclusion of this study and the suggestion for future work.

Chapter 2 Basic Theories for turbine system design

2.1 Fundamentals of Rankine Cycle^[2]

Rankine cycle is a mathematical model which is used to predict the performance of the steam engines. It is often in the range of around 42% for a modern coal-fired power station, and relatively less in solar thermal power plants since the scale is smaller and entrance temperature is lower.

1) Real power plant cycle (Superheat Rankine Cycle)

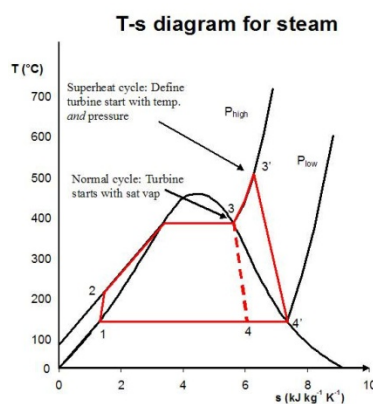


Figure 3. Super heat Rankine Cycle

In a real power plant cycle, the compression by the pump and the expansion in the turbine are not isentropic. In other words, entropy is increased during the two processes. This somewhat increases the power required by the pump and decreases the power generated by the turbine. In particular the efficiency of the steam turbine will be limited by water droplet formation. As the water condenses, water droplets hit the turbine blades at high speed causing pitting and erosion, gradually decreasing the life of turbine blades and efficiency of the turbine. To overcome this problem superheating steam is usually generated. On the Ts diagram above, state 3 is above a two phase region of steam and water so after expansion the steam will be very wet. By superheating, state 3 will move to the right of the diagram and hence produce a drier steam after expansion.

2) Heat Regenerative Rankine Cycle

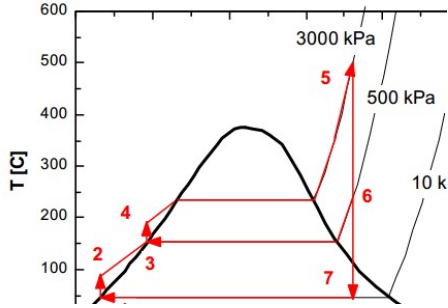


Figure 4. Regenerative Rankine Cycle

In regenerative Rankine cycle one or more feedwater heaters are used to preheat water emerging from the condenser. The Regenerative Rankine cycle (with minor variants) is commonly used in real power stations since it effectively raise the nominal cycle heat input temperature, by reducing the addition of heat from the boiler/fuel source at the relatively low feedwater temperatures that would exist without regenerative feedwater heating. This improves the efficiency of the cycle, as more of the heat flow into the cycle occurs at higher temperature. This process ensures cycle economy. For example, for an Rankine Cycle with initial parameters featuring 9MPa/500 °C with a backpressure of 4kPa, after the adoption of heat regenerative system, the cycle efficiency was improved by 12%^[23].

Feed water heaters come in two basic forms, one is the surface-type and the other is the contact-type. In the former type the extraction steam does not mix with condensate, the heater functions as an ordinary tubular heat exchanger. Whereas in the latter type, the condensate is mixed with the extraction steam (both at the same pressure) to end up with saturated liquid before the feed water pump. This process is called "direct contact heating". The deaerator is a typical contact-type of regenerative heater.

At present a combination of both types of feed water heaters are used in most plants. To illustrate the mathematical model of a regenerative system, here a five stage regenerative system for a 25MW coal fired power plant is used as an example.

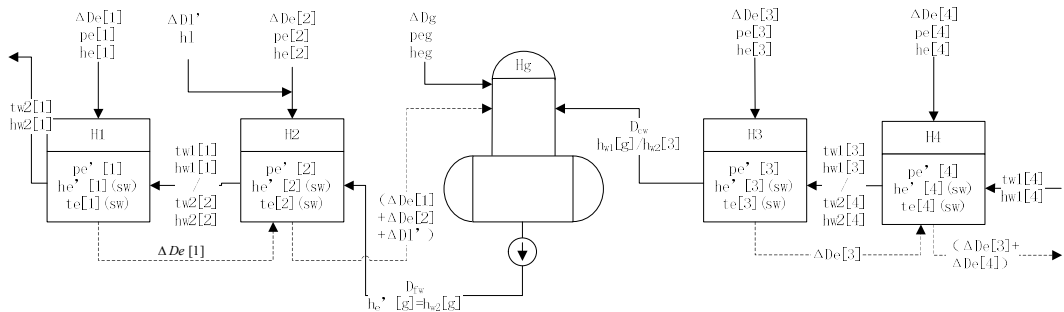


Figure 5. Mathematical model of heat regenerative system for 25MW power plant

As is shown in Fig.5 , the scheme include two high pressure regenerative heaters (near the boiler) and two low pressure regenerative heaters (near the condenser), a deaerator is placed in the middle owing to its special status. The connection scheme of drain

system is cascade drain flow.

The calculation usually starts with heater #1. Using energy conservation equation we obtain $\Delta D_e[1] = \frac{D_{fw}(h_{w2}[1] - h_{wl}[1])}{(h_e[1] - h_e[1])\eta_h}$, where $\Delta D_e[i]$, $h_e[i]$, $h_e'[i]$, $h_{wl}[i]$, $h_{w2}[i]$ representing the extraction steam flow rate, extraction steam enthalpy, drain enthalpy, inlet feed water enthalpy, outlet feed water enthalpy for heater i respectively, D_{fw} stands for mass flow rate of feed water, η_h represents thermal efficiency of heater i. For heater #2 since it receives drain from heater #1, in addition a flow of reclaimed shaft-packing leakage goes along with the extraction steam into the heater, in this case two additional income should be converted into equivalent extraction steam. The equations include:
 $\Delta D_e'[1] = \Delta D_e[1] \frac{h_e'[1] - h_e'[2]}{\Delta h_e[2]}$ and $\Delta D_l'' = \Delta D_l' \frac{h_e'[1] - h_e'[2]}{\Delta h_e[2]}$ respectively. Then energy balance is carried out in heater #2 as $\Delta D_e[2] = D_{fw} \frac{h_{w2}[2] - h_{wl}[2]}{\Delta h_{e2}\eta_h} - \Delta D_e' - \Delta D_l''$.

Since the working theory of deaerator involves both conservation of mass and energy, two simultaneous equations are listed as follows:

$$\text{Mass equation } \Delta D_g + \Delta D_e[1] + \Delta D_e[2] + \Delta D_l' + D_{cw} = D_{fw};$$

$$\text{Energy equation } \Delta D_g h_e[g] + (\Delta D_e[1] + \Delta D_e[2] + \Delta D_l') h_e'[2] + D_{cw} h_{wl}[g] = D_{fw} h_e'[g];$$

Solve the simultaneous equations and get $D_{cw}, \Delta D_g$. Then the rest of heaters can be analysed in the same way. The equations are listed as follows:

$$\text{Extraction flow rate of heater #3 } \Delta D_e[3] = \frac{D_{cw}(h_{w2}[3] - h_{wl}[3])}{\Delta h_e[3]\eta_h};$$

$$\text{Equivalent extraction steam } \Delta D_e'[3] = \frac{\Delta D_e[3](h_e'[3] - h_e'[4])}{\Delta h_e[4]};$$

$$\text{Extraction flow rate of heater #4 } \Delta D_e[4] = \frac{D_{cw}(h_{w2}[4] - h_{wl}[4])}{\Delta h_e[4]\eta_h} - \Delta D_e'[3];$$

In this way the extraction steam in each stage is calculated.

3) Rankine Cycle with reheat

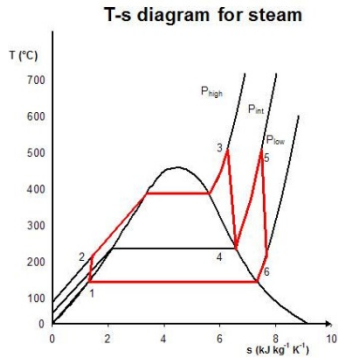


Figure 6. Rankine Cycle with reheat

The purpose of a reheating cycle is to remove the moisture carried by the steam at the final stages of the expansion process. In this variation, two turbines work in series. The first accepts vapor from the boiler at high pressure. After the vapor has passed through the first turbine, it re-enters the boiler and is reheated before passing through a second, lower-pressure, turbine. The reheat temperatures are very close or equal to the inlet temperatures, whereas the optimum reheat pressure needed is only one fourth of the original boiler pressure. Among other advantages, this prevents the vapor from condensing during its expansion and thereby damaging the turbine blades, and improves the efficiency of the cycle, given that more of the heat flow into the cycle occurs at higher temperature.

For a parabolic trough solar thermal plant, higher operation temperature results in two advantages for the power block. The main advantage is higher efficiencies as turbine inlet temperature increases. Another interesting consequence is the possibility of omitting a non-necessary steam reheating, which would not mean an efficiency increase. Steam reheating would be only necessary at lower turbine inlet temperatures, in order to avoid a great wetness fraction of steam at the turbine exhaust, which means a penalty in the turbine life-time, owing to the erosion of last steam turbine blades by water droplets. Besides that, the steam reheating integration would carry on several technological complications for this particular case; it is clear that the option of reheating directly in the solar field implies a complex configuration with high steam pressure drop; the alternative of using an auxiliary fired boiler means an additional natural gas consumption.

2.2 Basic theories for one dimensional turbine flow path design

In a steam turbine, high-pressure steam from the boiler expands in a set of stationary blades or vanes (or nozzles) and later result in high velocity. Then the high velocity steam strikes the set of moving blades. In this process, the kinetic energy of the steam is utilized to produce work on the turbine rotor. After stages of conversion, low pressure steam then exhausts to the condenser. The basic unit of producing work is a stage, a stage is composed of a set of stationary blades and a set of corresponding

moving blades.

2.2.1 The one dimensional flow theory

The preliminary design theory is based on a simplification of steady equilibrium adiabatic flow in the flow path which is in a reference frame rotating with the speed n (r/min). The basic equations include:

1) Continuity equation

$$\frac{dA}{A} + \frac{dc}{c} - \frac{dv}{v} = 0 \quad (1)$$

2) Energy equation

$$h_0 - h_1 = \frac{c_1^2 - c_0^2}{2000} \quad (2)$$

3) Process equation^[20]

$$s_0 = S(p, \frac{1}{\psi^2}(i - (\psi^2)i_{0w}^*)) \quad (3)$$

4) State equations

$$\frac{dp}{p} + \kappa \frac{dv}{v} = 0 \quad (4)$$

The core of preliminary stage design theory is a physical combination of the above mentioned basic equations and the velocity triangle theory. To design a turbine stage, a set of parameters are required:

- Mass flow rate G ;
- Rotational speed n ;
- Mean diameter of stage d_m ;
- Enthalpy distribution of stage Eh_i ;
- Velocity ratio of stage x_a ;
- Degree of reaction Ω_m ;
- Inlet flow angle α_1 ;
- Partial-arc admission degree e ;
- Data for cascade's velocity loss coefficients estimation;
- Data for additional energy loss computation: seal types and dimensions, radial and axial gaps dimensions, etc.

Denote the nozzle input section by 0, the nozzle output section by 1 in turbine stage. As to the rotor, denote the outlet section by 2. Then the process of turbine stage design can be carried out as follows^[24]:

- 1) Get Enthalpy drop in nozzle: $\Delta h_n = (1 - \Omega_m) \cdot \Delta h_t$ (kJ/kg), use h_0 and Δh_n to Find p_{lt} , v_{lt} in Mollier Chart.
- 2) Judge steam flow state at the outlet of nozzle using $\varepsilon_n = p_1 / p_0^*$, define the type of nozzle (Laval or convergent), choose α_1 .
- 3) Get nozzle outlet velocity: $C_1 = \varphi C_{lt}$ (m/s).
- 4) Acquire nozzle's outlet cross sectional area $A_n = \frac{GV_{lt}}{\mu_n C_{lt}} \times 10^4$ cm². Where μ_n stands for nozzle flow rate coefficient, semiempirically it is simplified to be only defined by degree of superheat or humidity. When $0.4 < \varepsilon_n < \varepsilon_{cr}$, a slight deflection occurs at the beveling part of the nozzle, in this case $A_n = \frac{G}{0.0648\sqrt{p_0/v_0}}$. The deflection angle can be calculated using

$$\sin(\alpha_1 + \delta_1) = \sin \alpha_1 \frac{V_{lt} c_{cr}}{V_{cr} c_{lt}} = \sin \alpha_1 \frac{\left(\frac{2}{k+1}\right)^{\frac{1}{k-1}} \sqrt{\frac{k-1}{k+1}}}{\varepsilon_n^{\frac{1}{k}} \sqrt{1 - \varepsilon_n^{\frac{k-1}{k}}}}.$$

- 5) Nozzle outlet height l_n and partial-arc admission degree e . When $\varepsilon_n > \varepsilon_{cr}$,
$$l_n e = \frac{A_n}{\pi d_m \sin \alpha_1}; \quad \text{when } 0.4 < \varepsilon_n < \varepsilon_{cr}, \quad l_n e = \frac{(A_n)_{\min}}{\pi d_m \sin \alpha_1}. \quad \text{Usually } l_n > 12 \sim 16 \text{ mm},$$

$$e > 0.15 \sim 0.3.$$
- 6) Nozzle loss can be calculated by $\Delta h_n = (1 - \varphi^2) \Delta h_n^*$ (kg/kJ), in which φ is the nozzle velocity coefficient. Using $h_1 = h_0 - \Delta h_n + \Delta h_{n\xi}$ and $p_{lt} = p(h_0 - \Delta h_n, s_0)$, inlet thermal dynamic point of the rotor blade can be acquired.
- 7) Define α_1 , then using velocity triangle theory $\beta_1 = \tan^{-1} \frac{c_1 \sin(\alpha_1 + \delta_1)}{c_1 \cos(\alpha_1 + \delta_1) - u}$, $w_1 = \frac{c_1 \sin(\alpha_1 + \delta_1)}{\sin \beta_1}$. Hence $\Delta h_{w1} = \frac{w_1^2}{2000}$, stagnation parameters can be acquired.
- 8) Enthalpy drop in the rotor blade $\Delta h_b = \Delta h_t \cdot \Omega_n$ (kJ/kg), stagnation enthalpy drop $\Delta h_b^* = \Delta h_b + \Delta h_{w1}$ (kJ/kg)
- 9) Get rotor blade outlet relative velocity $w_{2t} = 44.72 \sqrt{\Delta h_b^*}$, use graph.8 to acquire rotor blade velocity coefficient ψ .

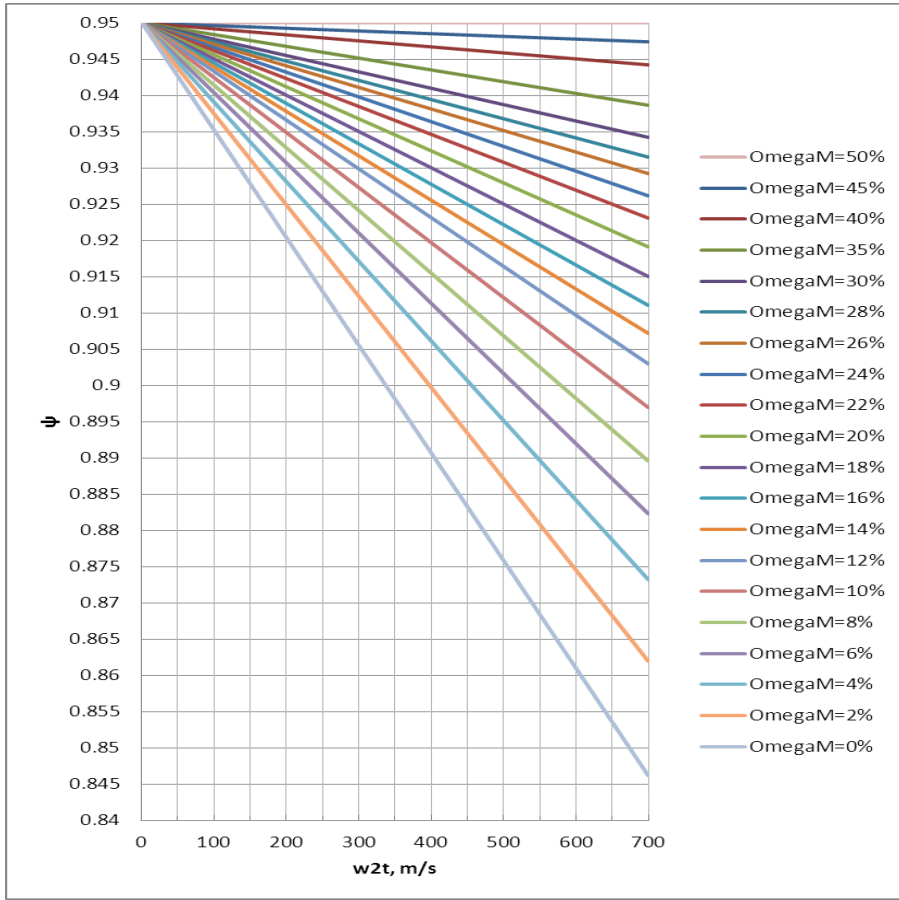


Figure 7. Relationship between ψ and Ω_m

- 10) Rotor blade loss can be simply calculated by $\Delta h_{b\xi} = (1 - \psi^2) \Delta h_b^*$ (kJ/kg). With the same process as nozzle calculation, steam thermal dynamic state point 2 can be found in the Mollier graph (h-s chart) using $\Delta h_{b\xi}$ and Δh_b .
- 11) Based on continuity equation, rotor blade exit area $A_b = \frac{GV_2}{w_2} \times 10^4$ (cm^2)
- 12) Rotor blade exit height $l_b^i = l_n + \Delta$. Hence relative outlet velocity angle $\beta_2 = \sin^{-1} \frac{A_b}{e\pi d_m l_b}$.
- 13) Using velocity triangle theory, obtain $\alpha_2 = \tan^{-1} \frac{w_2 \sin \beta_2}{w_2 \cos \beta_2 - u}$, $c_2 = \frac{w_2 \sin \beta_2}{\sin \alpha_2}$ (m/s).
- The complete velocity triangle of a stage can be drawn.
- 14) Carryover loss $\Delta h_{c2} = \frac{c_2^2}{2000}$ (kJ/kg)
- 15) Wheel periphery enthalpy drop $\Delta h_u' = \Delta h_{c_0} + \Delta h_t - \Delta h_{n\xi} - \Delta h_{b\xi} - \Delta h_{c_2}$

16) Efficiency of the wheel periphery $\eta_u = \frac{\dot{E}_u}{\dot{E}_0}$

17) Wheel periphery power produced by 1 kg steam $W_u = \frac{u}{1000} (c_1 \cos \alpha_1 + c_2 \cos \alpha_2)$

18) Efficiency of the wheel periphery $\eta_u = \frac{W_u}{\dot{E}_0}$

19) Check $\Delta \eta_u = \frac{|\dot{\eta}_u - \eta_u|}{\dot{\eta}_u} \times 100\%$; recheck previous calculation if $\Delta \eta_u > 1\%$.

20) Calculation of other forms of losses: $\Delta h_l, \Delta h_f, \Delta h_p, \Delta h_e, \Delta h_x$ etc.

21) Stage efficiency $\eta_i = \frac{\dot{E}_u - \Delta h_l - \Delta h_f - \Delta h_p - \Delta h_\delta - \Delta h_e - \Delta h_x}{\dot{E}_0}$

For a typical dual row governing stage, the design process is almost the same except for an addition of another pair of velocity triangles. That is to say, due to the existence of another set of entrance bucket and rotor blade, the computational complexity is twice of a regular one. A simplified illustration of calculation for this type is shown in Fig.8.

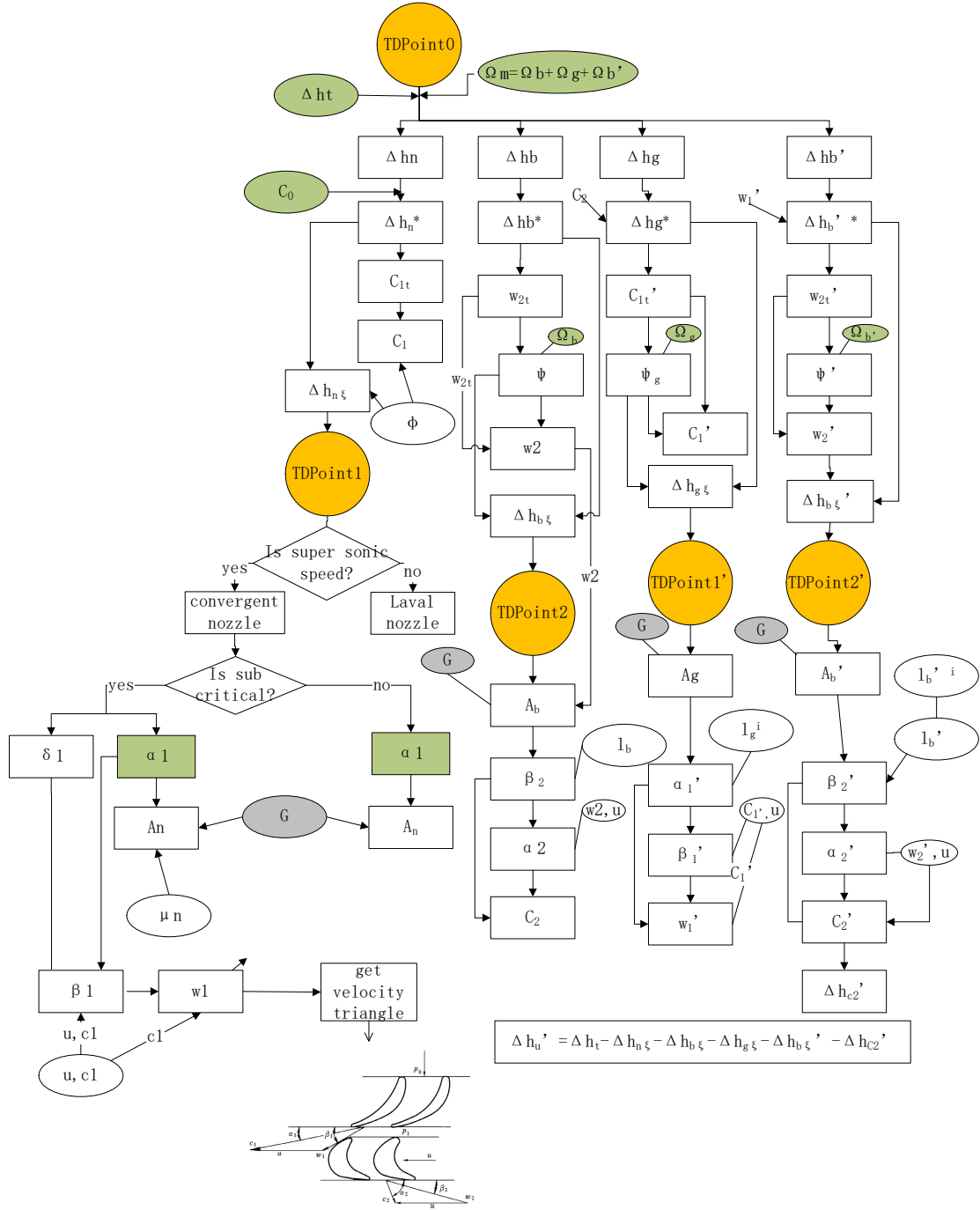


Figure 8. Calculation process for a dual row governing stage

2.2.2 Extra Loss models

In this study, six types of extra losses are considered. Based on Steam turbine course design material by Feng Huiwen^[24], the mathematical models are chosen as follows:

- Losses related to blade height: $\Delta h_l = \frac{a}{l} \times \Delta h_u'$;
- Friction and ventilation losses: $\Delta h_f = 1.07 \times d_b^2 \left(\frac{u}{100} \right)^3 / (Gv_2)$;

- Baffle leakage losses: $\Delta h_p = \frac{\pi \delta_p d_p}{A_n \sqrt{z_p}} \times \Delta h_u$;
- Blade tip losses: $\Delta h_{pt} = \frac{\mu_\delta \delta_m \psi_t}{\mu_t \sin \alpha_1} \Delta h_u$;
- Losses due to partial-arc admission: $\Delta h_e = \frac{E_0 x_a}{e} [K_e x_a^2 (1-e) + K_e' \frac{Z_m}{d_b}]$;
- Humidity losses: $\Delta h_x = (1 - \frac{x_1 + x_2}{2}) \Delta h_u$;

Where a , K_e , K_e' , μ_δ , ψ_t , μ_t are empirical coefficients, l stands for blade height, Δh_u is rim enthalpy drop, d_b is mean line diameter of rotor blade, u is rim velocity, G is mass flow rate of the stage, v is the specific volume of stage outlet point, δ_p is size of diaphragm air gap, d_p is the diameter of diaphragm, z_p is the tooth number of shaft seal, δ_m is the average axial air gap size of blade tip, α_1 is the steam inlet direction angle, E_0 is the ideal energy of the stage, e is partial-arc admission degree, Z_m is nozzle set number, x_1, x_2 are dryness fraction of stage inlet and outlet point respectively.

For calculations, all corrections in the formulas are taken from graphs, and are entered as the charts, then computed by linear interpolation on one or two independent variables.

Chapter 3 Optimization

3.1 Objectives

The key to an optimized scheme lies in the enthalpy drop distribution of stages. Meanwhile for an integrate steam turbine design process, other considerations must be taken into account while stage distribution since the extraction points must coincide with each post stage points. Existing literatures obviously put most emphasis on describing each elementary theory, whereas interactions between these procedures were vaguely described. For example in both Feng and Xiao's literatures, interaction between heat regenerative system design and stage distribution design is merely described as "if post stage points and extraction points don't coincide with each other, adjustment should be made". To obtain the best stage division scheme as well as following the constraint of "coincident points", a new design phase (also used as the optimization phase) is proposed and described in this chapter.

3.2 Optimization Model

The basic idea of the optimization method is to generate a solution range using each extraction point and its corresponding post stage point as minimum and maximum boundaries, let the program randomly select a mutual point within the range as the final solution, then carry out inverse calculations for stage distribution and heat regenerative system respectively using the selected mutual point. Hence using the new distributions of the two above-mentioned systems, stage by stage calculation can be carried out, resulting in a final solution. Since this process can be carried out for many times using a cycle counter, a variety of paralleled calculations can be generated and compared, using turbine internal efficiency as a final index, best solution can be chosen. It is in this way that both best global internal efficiency and coincident points are achieved.

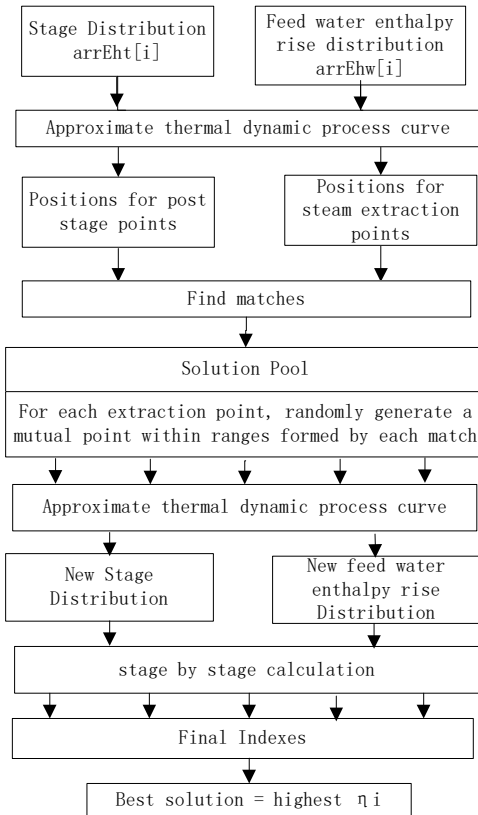


Figure 9. Optimization algorithm

3.3 Methodology

The added optimization phase is entitled “Coupling” in this research. The realization of coupling method can be divided into three forms, one is based on post stages points, the other is based on extraction points and the third concerns both extraction points and stage points.

3.3.1 Coupling based on (fixed) post stage points

Coupling based on (fixed) post stage points means that when mismatching happens, the extraction points take initiatives to change in a range, until mismatching disappears.

The algorithm is shown in the following flow chart:

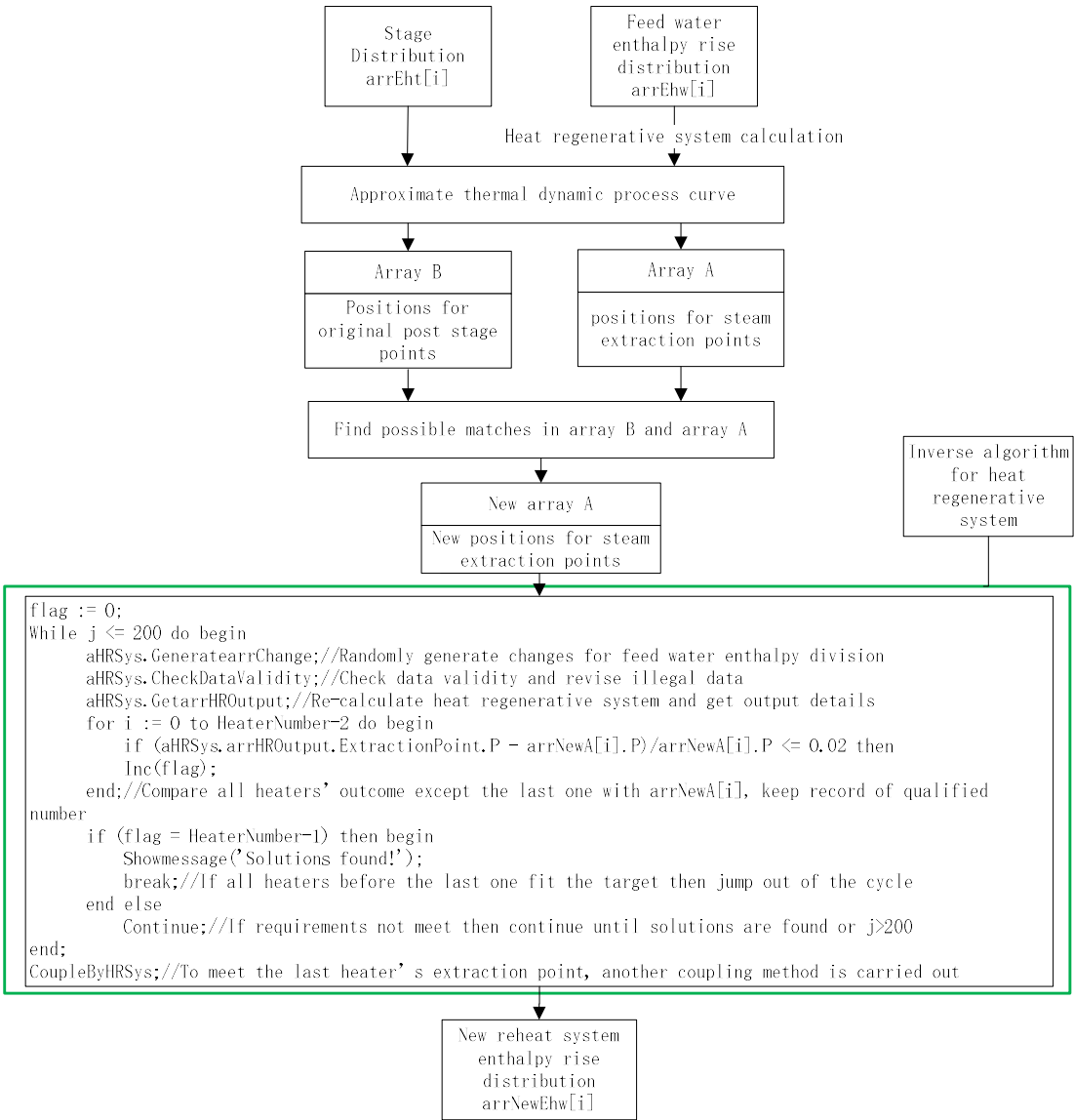


Figure 10. Coupling based on fixed post stage points

Rigidly speaking, this coupling method does not rely on fixed post stage points completely. The reason lies in the constraint of total feed water enthalpy rise. Fig. 10 is a simple example to illustrate this phenomenon.

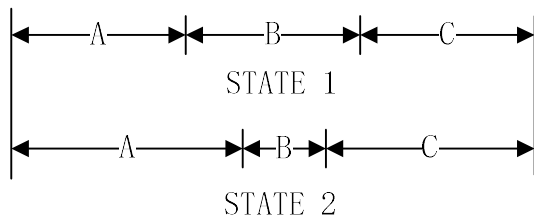


Figure 11. Illustration of coupling based on fixed post stage points

As shown in Fig 10, A, B, C are originally three equal length line sections. Their total length is a constant value. in state 2 for some reasons Line section A increases its

length by ΔA , B decreases its length by ΔB , hence C has to increase by $(\Delta B - \Delta A)$ to maintain the total length. In the same way, since the regenerative heaters are not completely independent from each other, one of the heaters has to shoulder the changes brought by other heaters. Due to this fact there would always be a passive heater. For convenience, in algorithm design the last stage of heater is deemed as a default ‘passive heater’. To deal with the ‘passive heater’ matching problem, another simpler coupling method – coupling based on extraction points is then used.

3.3.2 Coupling based on (fixed) extraction points

This type of coupling concerns setting extraction points as revise goals for stage distribution. The first step is to locate point positions in both sides on a benchmark – in this case the approximate thermal dynamic process curve. Then after a comparison between points from both sides, based on each extraction point position a closest post stage point is found and then changed into the same position as its extraction correspondent. Finally a re-scheme of stage distribution is carried out. This process involves inverse calculation base on stage division theory. The detailed algorithm is shown in the following chart:

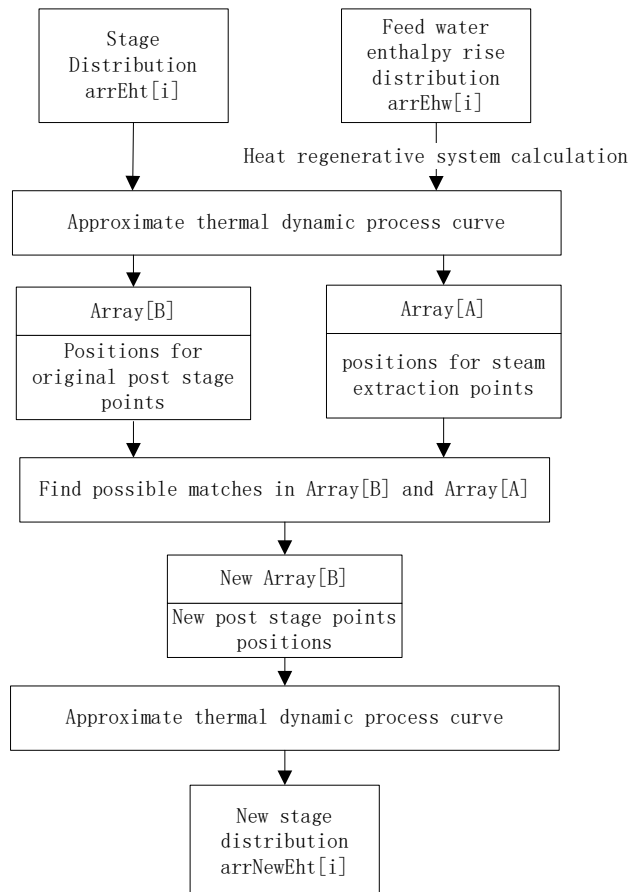


Figure 12. Coupling based on extraction points

3.3.3 Coupling based on both extraction points and post stage points

Coupling based on both extraction points and post stage points means the solution is found on the basis of both sides of points. In this method each pair of possible match (one from post stage points array the other from extraction points array in each pair) is found and a selection range is formed between the two points. After automatically defining the ranges (the number of ranges equals to the number of extraction points, due to the reason that number of regenerative heaters is always less than that of turbine stages), the program will randomly choose a point within each range and set the chosen point as the coincidence point. Then two inverse algorithms are carried out respectively for heat regenerative system design phase and the stage division phase.

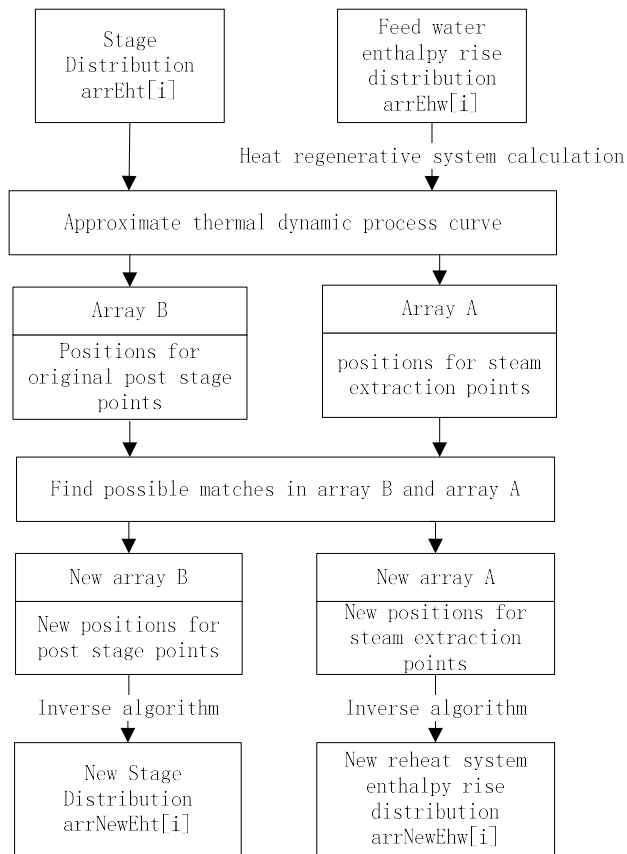


Figure 13. Coupling based on both sides of points

Based on this algorithm, a solution generator is utilized to generate several groups of possible matching solutions, the global efficiency index η_i is then used to filter the best solutions. The algorithm for optimization process is demonstrated as follows:

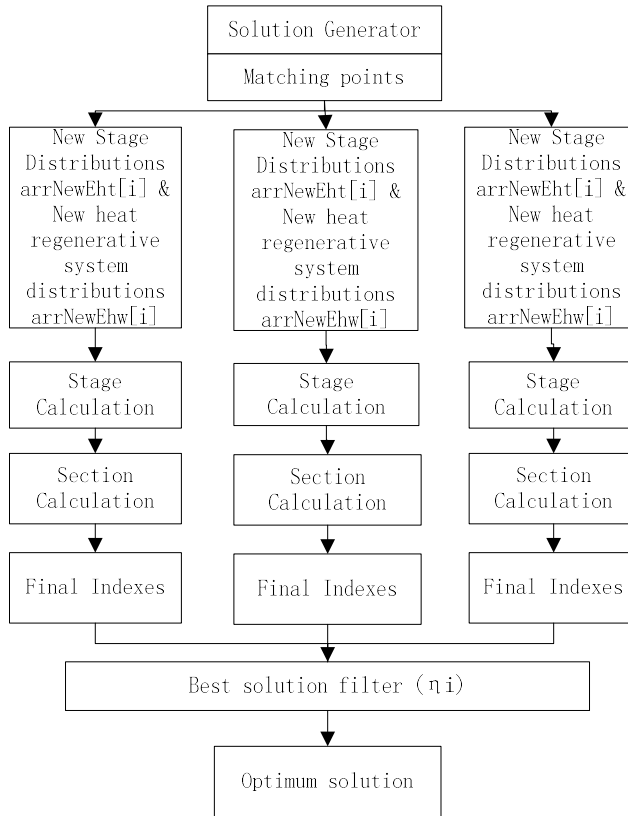


Figure 14. Algorithm of the optimization process

3.4 Tests and conclusions

The adoption of coupling method helps to determine the suitable adjustment in enthalpy drops in both stage distribution and heat regenerative system. To illustrate its functions, a condensing turbine with a two-stage regenerative system is designed and studied using STFPD.

3.4.1 Case Settings

The design point in this case is shown in table 4 below.

Table 4. Design Point parameters in this case

<i>Turbine</i>	
Isentropic efficiency	0.61
Electro-mechanical efficiency	0.98
<i>Condenser pump</i>	
Outlet pressure (MPa)	1.2

Feedwater pump

Outlet pressure (MPa)	6.3
-----------------------	-----

Deaerator

Pressure (MPa)	0.515
----------------	-------

Condenser

Pressure (MPa)	0.006
----------------	-------

Fig.14 below demonstrates initial settings for this case.

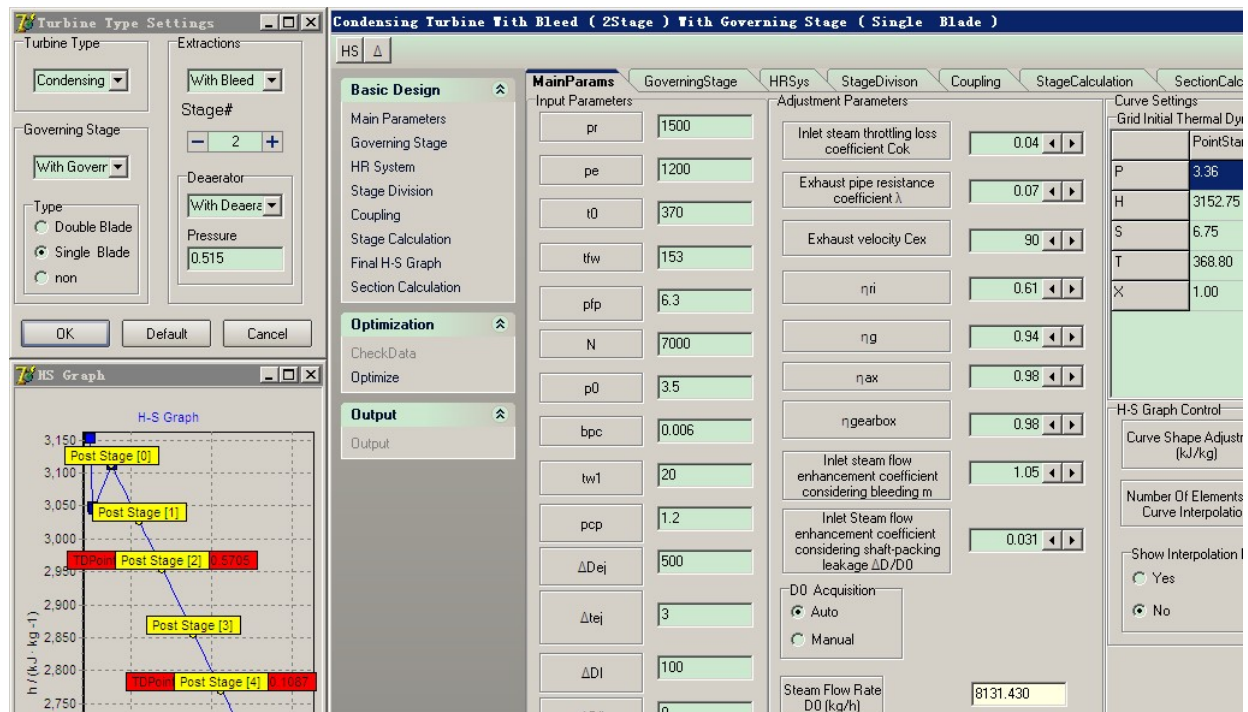


Figure 15. Initial settings

Under the same initial conditions, two tests were carried out respectively to show the effectiveness of the optimization phase. Table 5 below shows the details and purposes for setting these cases.

Table 5. Operations for each case

Case	Operations
------	------------

1 Auto coupling based on both extraction points and post stage points

2 Manual calculations

3.4.2 Results and comparisons

Table 6. Case 1_Stage enthalpy drop distribution and its final indexes

Z	1	2	3	4	5	6	7
Eht(kJ/kg)	104.18	125.61	121.51	139.67	154.88	187.00	276.14
Dm(mm)	501.00	522.34	546.28	572.81	601.94	633.67	668.00
Xa	0.362	0.383	0.374	0.372	0.377	0.383	0.390
η el				25%			
η i				66%			
Pi(kw)				1234.57			

Table 7. Case 2_Stage enthalpy drop distribution and its final indexes

Z	1	2	3	4	5	6	7
Eht(kJ/kg)	177.22	146.39	183.99	153.82	166.34	141.31	138.09
Dm(mm)	501.00	522.34	546.28	572.81	601.94	633.67	668.00
Xa	0.308	0.354	0.330	0.379	0.383	0.437	0.466
η el				25%			
η i				61%			
Pi(kw)				1194.42			

With a uniform initial parameter set, under the same scheme of stage number and meanline diameter distribution, internal efficiency of case 1 is $(0.66-0.61)/0.61*100\% = 8.2\%$ higher than case 2. Hence it is obvious from the comparison of case 1 and case 2 that the adoption of a optimization method has a great impact on rapidly generating good solutions.

In addition, from the final curve it can be seen that thanks to coupling, the extraction pressure fits well with the real post stage thermal dynamic point pressure, which means the final iteration work is reduced to changing the enthalpy of extraction point only.

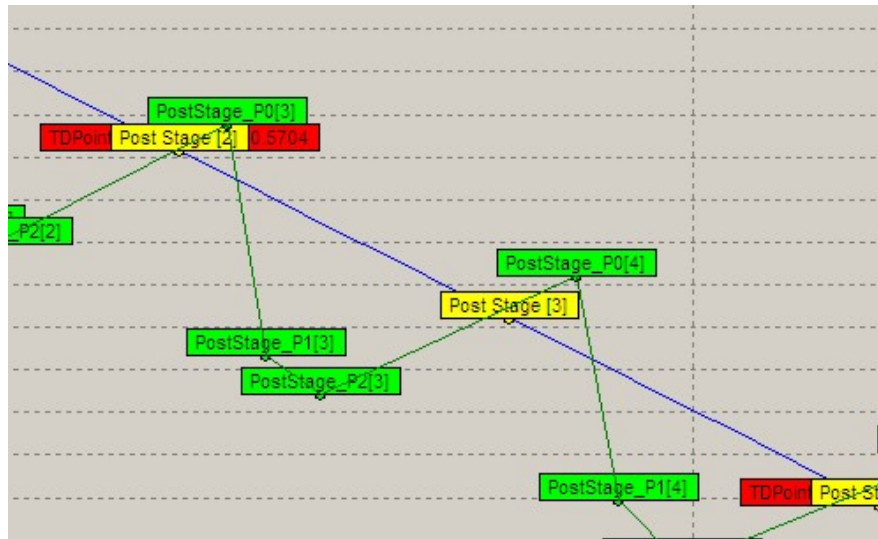


Figure 16. Final curve of case 1

3.4.3 Conclusions

In this chapter, a new standard process which is beneficial to both reducing unnecessary iterations as well as providing possible optimized results is brought up. The results were compared to a set of manual calculations and the results further proved the advantages of this method.

Chapter 4 Establishment of STFPD (Steam Turbine Flow Path Design) software platform

4.1 Methodology

4.1.1 Requirements analysis

In software engineering, the first and most important step is the requirements analysis. Requirements are capabilities and conditions to which the system (and more broadly, the project) must conform^[24]. The purpose of requirements is:

- To provide system developers with a better understanding of the system requirements.
- To define the boundaries of (delimit) the system.
- To provide a basis for planning the technical contents of iterations.
- To provide a basis for estimating cost and time to develop the system.
- To define a user-interface for the system, focusing on the needs and goals of the users.

According to Li Wei^[23], 40%~60% problems are related to insufficient requirements analysis. Hence it is important to get well informed and make adequate preparation before start coding.

Also in the development of engineering design software it is of vital importance to guarantee that the programmer has a full understanding of the problem to be solved, and is able to make design decisions during the process of coding. For this type of work, in a certain degree, understanding of the problem itself is much more important than knowledge and experience of programming^[25].

To conclude, it is of vital importance to get full understanding of the problem and make adequate requirements analysis.

This study mainly concerns designing a specific steam turbine system (megawatt level, available for solar thermal power plants), to define the scope of work in detail, several points must be considered:

Firstly, the type of the steam turbine. Steam turbines generally come in two types: axial type and radial type. The basic design theories differ from each other in a certain extent. Despite the fact that the efficiency of radial turbine is higher than the corresponding axial steam turbine, technology of the latter is still more mature, hence only axial type is considered in this paper. Under the framework of axial steam turbine, detailed types of steam turbine need to be chosen. These features include: whether it is an impulse or reaction turbine, whether it is a condensing or backpressure one, whether it has

governing stage or not, and a rough set of initial parameters should be given.

Secondly, general design of heat regenerative system. This step mainly concerns whether to integrate a heat regenerative system or not, as well as the number of heaters (if necessary).

Compared to a reaction turbine, an impulse turbine usually has slightly lower efficiency and produces much higher work. Due to that reason impulse turbines are preferable since the number of stages for an impulse turbine is less than a reaction one, in this way production cost is decreased. As to other options mentioned, choices can be left for users to decide.

Hence the scope of work is confined to designing a condensing/back pressure turbine with user choice of governing stage, extraction system and reheat system (see Fig. 16).

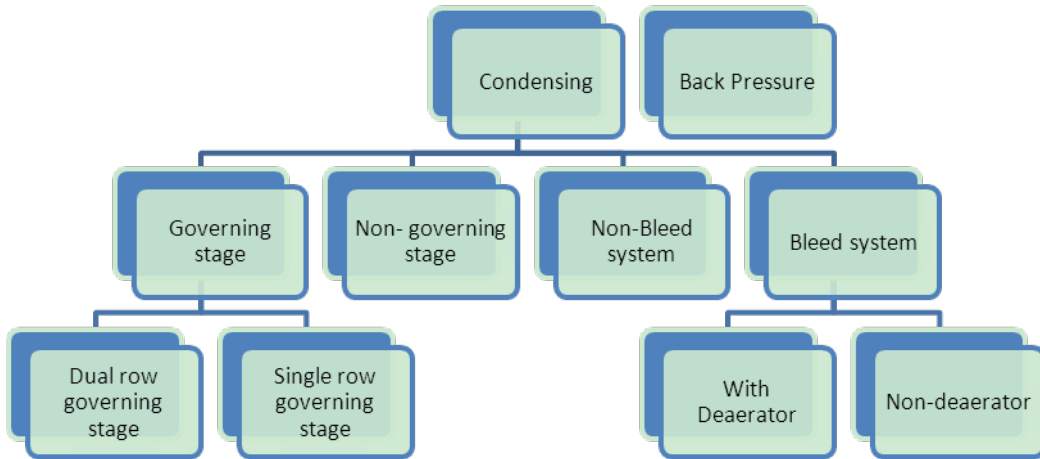


Figure 17. Scope of work

4.1.2 Programming paradigms

Modern programming languages include two paradigms, one is procedural and the other is object-oriented. The former paradigm is essentially an abstraction of machine/assembly language. A program written by procedural paradigm is organized around procedures. This type of program focus on data structures, algorithms and sequencing of steps. A procedural program usually consists of a collection of variables, each of which at any stage contains a certain value (a number, a character, a string of characters, etc), a collection of statements that change the values of these variables. The building-block of this type program is the procedure or function. Advantages of procedural programming include: Clear separated procedures and data, rigid transformation of concepts between analysis and implementation. The disadvantages lie in the long step between design models and implementation, also since the procedures are often hard to reuse, programs written in this type of paradigm are often hard to extend and maintain.

In the paradigm of OOP (object-oriented programming), an object refers to an entity with a well-defined boundary and identity that encapsulate state and behavior in which state is represented by attributes and relationships, behavior is represented by operations, methods, and state machines. A type or class is always used to classify a category of similar objects. Since objects of the same class have the same data elements and methods, codes are more agile and reusable. Objects send and receive messages to invoke actions. Compared to procedural programming, advantages of object-oriented programming include facilitates architectural and code reuse, models more closely reflect the real world, more accurately describes corporate entities, decomposed based on natural partitioning and easier to understand and maintain Stability. Also, in this structure a small change in requirements does not mean massive changes in the system under development, indicating its adaptivity to change.

A modern object-oriented programming system can be used to present large, complex programs to user in a simple way, providing good feedback and allowing rapid use. For a typical engineering design process which is usually iterative, it is particularly valuable.

The turbine flow path designing process is a calculation-centered process which generates hundreds and thousands of parameters along the way of ‘designing’. The easiest way of realizing the design is through procedural oriented programming, as is demonstrated in the study of ‘Source code attached to Turbine Course Design’. Yet it is clear that behind the convenience of coding, there is a sacrifice of user convenience. Since interactions between the user and the program are frequently asked for during the process of design, well performed GUI (Graphical User Interface) is in desire. In this study, a more efficient and more user friendly approach is developed using Borland Delphi. Embarcadero Delphi is an integrated development environment (IDE) for console, desktop graphical, web, and mobile applications. It was originally developed by Borland as a rapid application development tool for Windows^[2]. It stands out with its own privileges by providing various visual components and events easily contribute to GUI. Because Delphi itself is developed based on object oriented programming paradigm, to make the most of this IDE tool, an innovative combination of design algorithm and OOP paradigm is used while coding.

4.2 General description of STFPD

4.2.1 General introduction

The program of STFPD (Steam Turbine Flow Path Design) is specialized for designing small and medium sized industrial steam turbines. It consists of 28 unit modules which cover all the functions required in preliminary design.

In STFPD, typical design process starts with turbine type settings. As can be seen from Fig.17, it gives users a range of capabilities to rapidly select major form of a turbine system which includes the turbine type, general information on the governing stage,

basic options on steam regenerative system such as number of regenerative heaters and choices on deaerator.

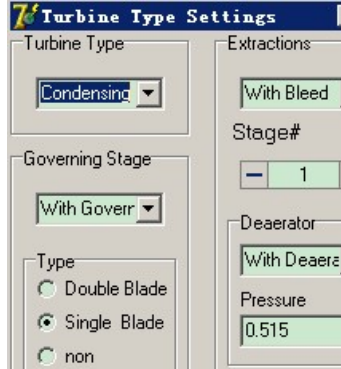


Figure 18. STFPD: Turbine Type Settings

After type settings of turbine system, press OK button to enter the main work space of STFPD (Fig.18). The program would automatically records the choice made in last design phase and arranges correspondent visual components of the next phase. In this case, since a condensing turbine with one bleed and a single governing stage is chosen in the type settings phase, the specific type is shown as the caption of the main work space form.

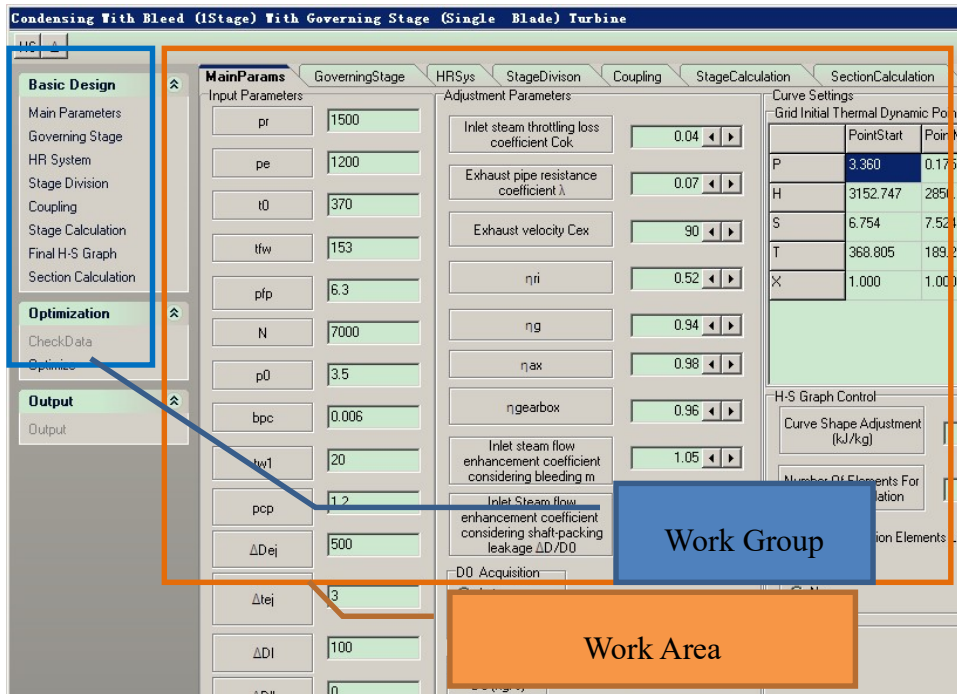


Figure 19. STFPD: Main Work Space

As is shown in Fig.18, the main work space is composed of two major parts: the work group and the work area. The part of basic design includes the standard design procedure: Main parameters input and analysis, governing stage design, heat regenerative system design, stage division, coupling of extraction point and stage

division, stage by stage design and calculation, draw final H-S graph and section calculation. The optimization part includes data checking and optimize algorithm. Finally the output workgroup record and print out the results. Each item in a workgroup has a corresponding tabpage shown in the work area.

Since the design process is a progressive one, at the beginning the database is not fully established yet, so in the first round of design, the tabpages are designed to be in function in a certain order. To be more specific, when first design a procedure must be rigidly followed in the sequence of (see Fig.19):

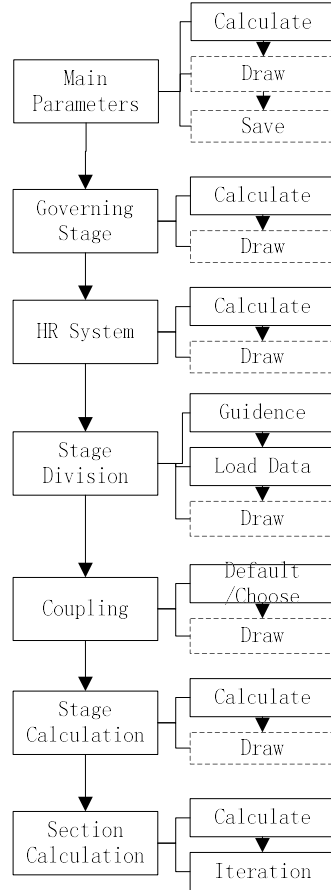


Figure 20. STFPD: Progressive Design in the first round

When finishing the first round of design, the initial approximate curve no longer fits the design status, due to unforeseeable losses changes the post stage points (increases or decreases along the equipressure line). Though maintaining more or less the same pressure, extraction points still dispart the post stage points. Hence another round of coupling should be carried out. This time only coupling by post stage is allowed to avoid complex situations caused by dramatically changing the near-mature stage conditions. To conclude, the iteration process concerns a cycle of ‘Checking coincidence’ → ‘coupling based on post stage points’ → New round of ‘stage calculation’. Fig.20 shows the algorithm for iteration.

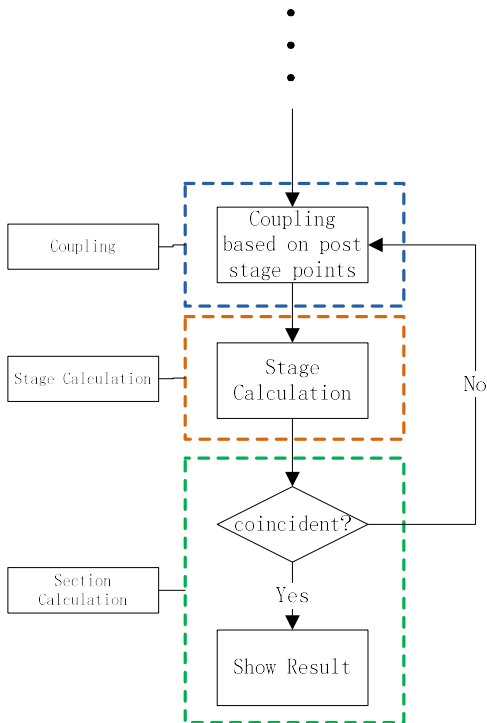


Figure 21. Algorithm of iteration

4.2.2 Module Introduction

1) Module ‘MainParams’

Main parameters (analysis) module acts as a guide to collect initial data for a steam turbine. After ‘Input Parameters’ and ‘Adjustment Parameters’ are given, press Calculate button on the right side, Steam flow rate D0 and initial thermal dynamic points are automatically calculated and shown in the blankets (Fig. 21). The initial thermal dynamic points are processed points representing the actual inlet and outlet point for the turbine, a third point (PointMid) is generated according to the h-s chart control information set by the user.

MainParams		
Input Parameters		
pr	1500	
pe	1200	
t0	370	
tfw	153	
pfp	6.3	
N	7000	
p0	3.5	
bpc	0.006	
tw1	20	
pcp	1.2	
ΔDej	500	
Δtej	3	
Adjustment Parameters		
Inlet steam throttling loss coefficient Cok	0.04	◀ ▶
Exhaust pipe resistance coefficient λ	0.07	◀ ▶
Exhaust velocity Cex	90	◀ ▶
η_{ri}	0.52	◀ ▶
η_g	0.94	◀ ▶
η_{ax}	0.98	◀ ▶
$\eta_{gearbox}$	0.96	◀ ▶
Inlet steam flow enhancement coefficient considering bleeding m	1.05	◀ ▶
Inlet Steam flow enhancement coefficient considering shaft-packing leakage $\Delta D/D_0$	0.031	◀ ▶
D0 Acquisition		
<input checked="" type="radio"/> Auto		
<input type="radio"/> Manual		
Curve Settings		
Grid Initial Thermal Dynamic Points		
	PointStart	PointMid
P	3.360	0.175
H	3152.747	2850.287
S	6.754	7.524
T	368.805	189.202
X	1.000	1.000
H-S Graph Control		
Curve Shape Adjustment (kJ/kg)		
Number Of Elements For Curve Interpolation		
Show Interpolation Elements List		
<input type="radio"/> Yes		
<input checked="" type="radio"/> No		

Figure 22. Main Params (analysis) module

When pressing Draw button, an approximate thermal dynamic process curve is drawn and shown based on three point interpolation of the initial thermal dynamic points (Fig. 22).

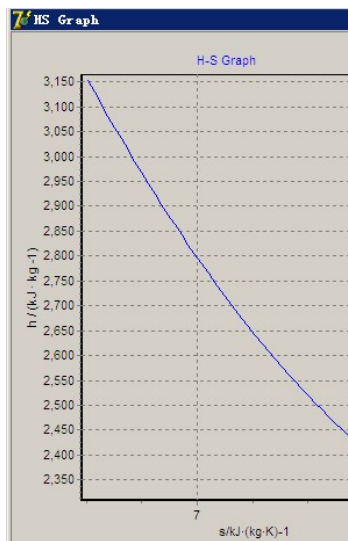


Figure 23. h-s Chart

Module ‘MainParams’ also includes a data saving/loading function which allows users keep record of last changes in the initial data.

2) Module ‘Governing stage’

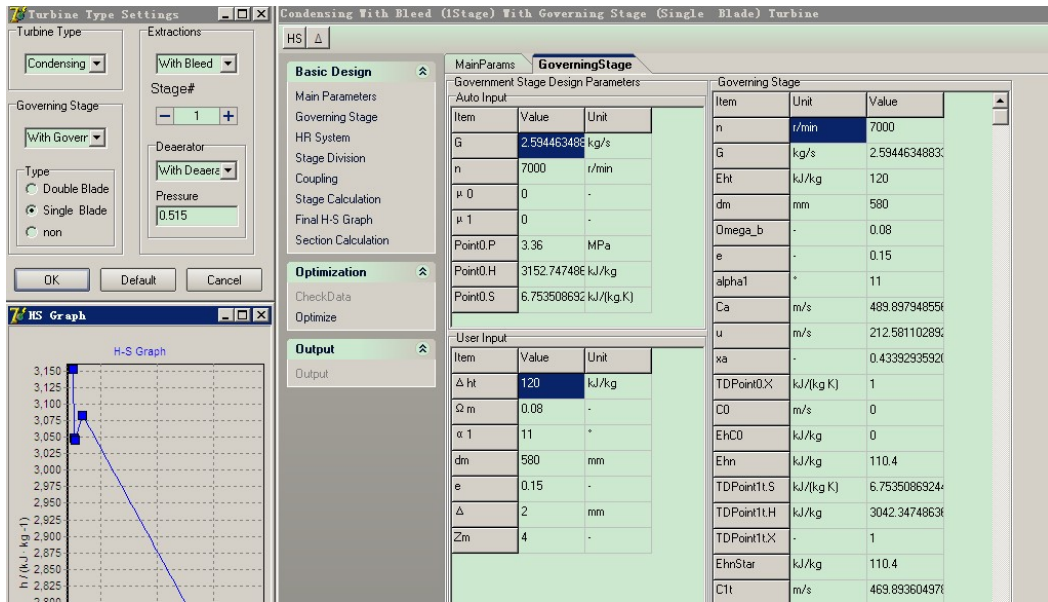


Figure 24. Module 'Governing Stage'

Module 'Governing Stage' is used to design a governing stage. The input parameters are classified into two groups: the automatic ones and the manual ones. Users have freedom to adjust manual input parameters and though 'Calculate' button acquire the whole design information for a governing stage. After acquiring governing stage results, a new approximate thermal dynamics process curve can be drawn (see left side of Fig. 23.).

3) Module 'HRSys'

The module 'HRSys' focuses on the design of heat regenerative system. The number of heaters corresponds to the initial settings in the first step, namely the 'Turbine Type Settings'. In Fig. 24, a two-stage regenerative system is shown.

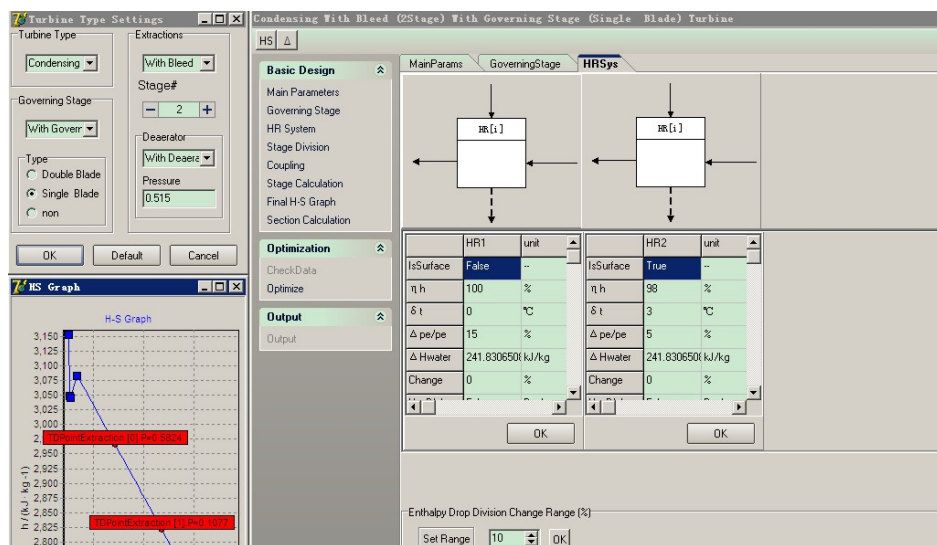


Figure 25. Module 'HRSys'

For each heater, user need to set the type of heater (surface or contact), efficiency of the heater, terminal temperature difference, pressure loss of extraction steam, feed water heat drop division and its control index ‘Change’, last but not least, a Boolean index ‘HasDlaIn’ controlling the setting of reclaimed shaft-packing leakage. Moreover, a small change range can be set by the user to control the heat drop division of regenerative system. As for this aspect, generally an average division rule is applied, yet according to Wang Naining^[10], a small deviation range of 10%~20% is allowed during heat drop division. Since the change in heat drop barely affects the global thermal efficiency, but is meaningful for the coupling of heat regenerative system division and stage division, hence the trick is applied here.

After clicking calculation button, every detail of the heat regenerative system is acquired thanks to the data processing module. Click ‘Draw’ button and the steam extraction points are visible in the h-s Chart. As is picturized in Fig. 24.

4) Module ‘StageDivision’

This module is used to generate stage division results including the number of stages and the enthalpy drop of each stage. Also a rough formation of stage mean line shape and velocity ratio for each stage can be settled since the enthalpy drop is directly

$$\text{related to } dm \text{ and } xa \quad (\Delta h_i[i] = \frac{Ca[i]^2}{2000} = \frac{(\pi d_m[i]n)^2 / x_a[i]^2}{2000} = \frac{\pi^2 d_m[i]^2 n^2}{2000 \times 60 \times x_a[i]^2}).$$

One can go through the stage division process via either manual or automatic method by checking or unchecking the ‘Manual checkbox’. Here the automatic approach is recommended since it is more reliable with a set of rigid data analysis process based on empirical design.

To make most use of automatic design function, user can click on the ‘guidance’ button. A new form entitled ‘StageDivRef’ is shown. After going through variable arrangements, click Calculate button to generate results, this process can be repeated until satisfying results are acquired. Then press ‘save’ button and exit the interface.



Figure 26. ‘StageDivRef’ sub-module

Back to the main form press ‘Load Data’ Button to fill in the results generated by the sub form. Grid ‘Enthalpy Drop Division Reference’ is then filled with stage division information (including stage number Z, ideal enthalpy drop Eht, mean line diameter dm and velocity ratio xa).

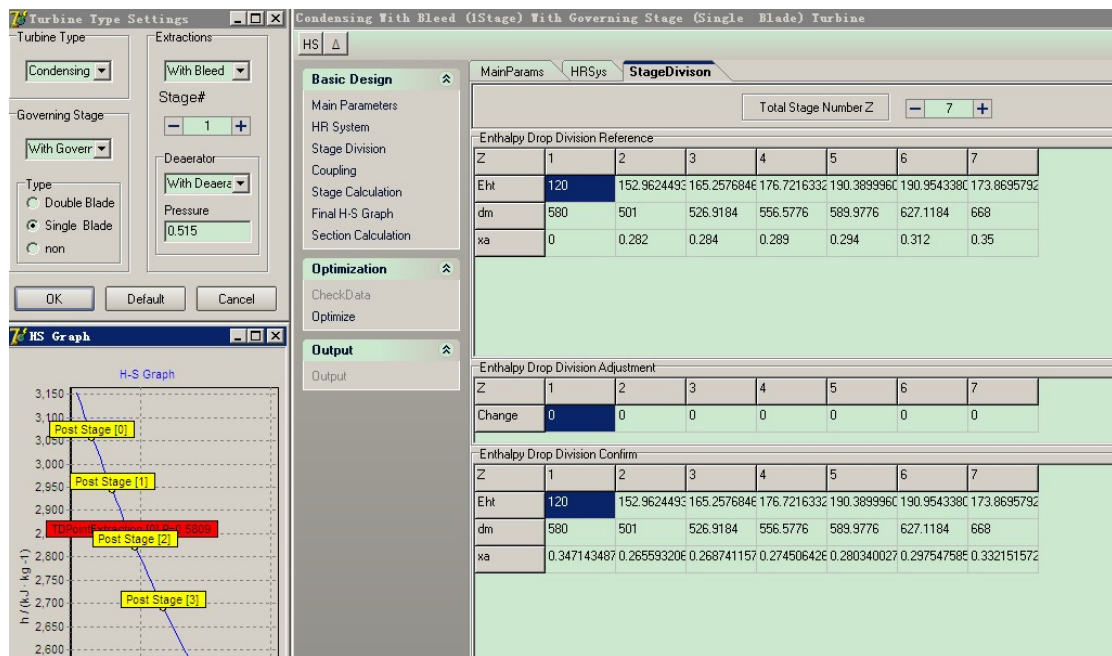


Figure 27. ‘StageDiv’ Module

Input enthalpy drop adjustment information and click ‘OK’ button hence we get the

final ideal enthalpy drop information. Press ‘Draw’ button the division situation is shown on the h-s chart (see the yellow labeled post-stage points).

5) Module ‘Coupling’

The ‘Coupling’ module is used to couple the stage division result and the heat regenerative system division result. When heater number in heat regenerative system is one, only coupling based on heat regenerative system can be used (since the feed water enthalpy rise is a fixed number). After picking up a coupling method, press ‘Confirm Base’ and then ‘Calculate’ button, a new array of coincident post stage points and extraction points are generated. Use ‘Draw’ button to visualize results of new division.

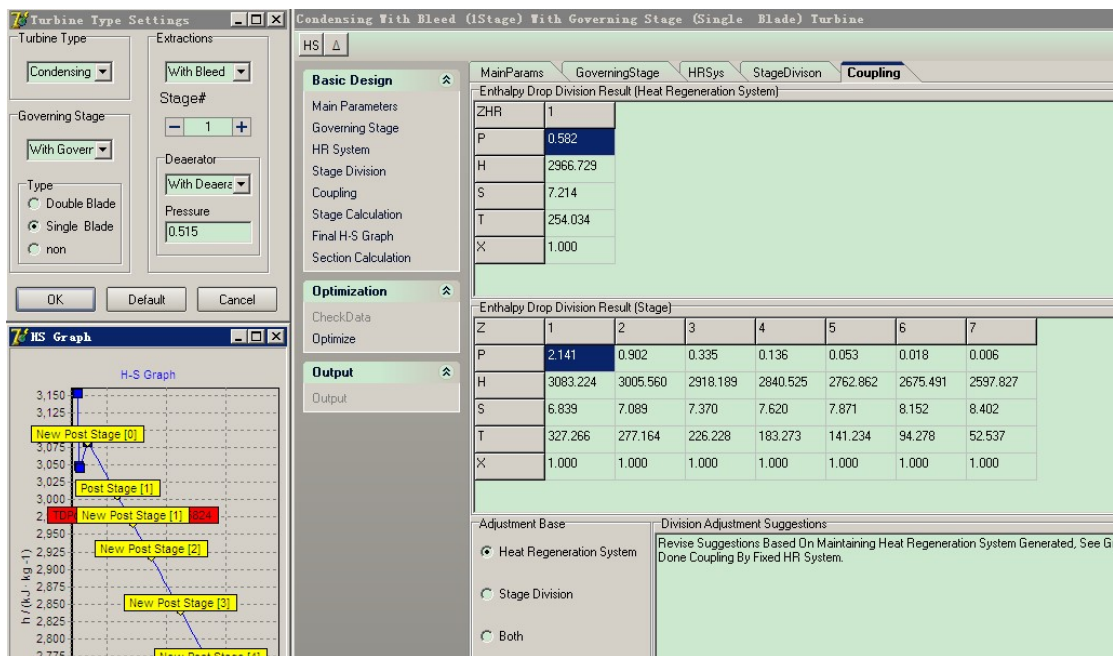


Figure 28. Module 'Coupling'

6) Module ‘Stage Calculation’

Module ‘Stage Calculation’ is carried out the same way as module ‘Governing stage’. Two lists of both automatic and manual inputs are shown at first, after users’ adjustment, the ‘Calculate’ button leads users to a new sub module named ‘Stage Calculation Results’ in which specific design results of both governing stage and pressure stages are demonstrated.

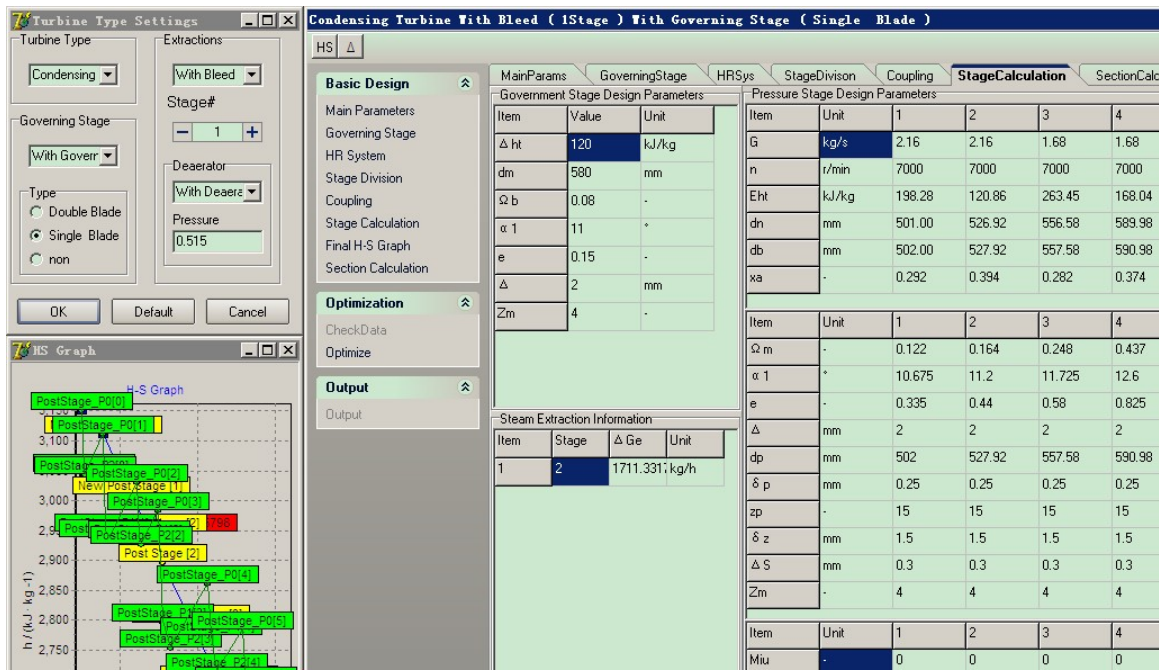


Figure 29. Module 'Stage Calculation'

Demonstration of sub module ‘Stage Calculation Result’ is shown in the picture below.

Governing Stage			Pressure Stage				
Item	Unit	Value	Item	Unit	1	2	3
n	r/min	7000	G	kg/s	2.56668571056	2.0086458947	2.0086458947
G	kg/s	2.5944634883	n	r/min	7000	7000	7000
Eht	kJ/kg	120	dn	mm	501	533.9825	572.81
dm	mm	580	db	mm	502	534.9825	573.81
Omega_b	-	0.08	Eht	kJ/kg	297.860715191	191.352016425	221.42803831
e	-	0.15	xa	-	0.2383849138	0.3169601902	0.3160337546
alpha1	*	11	OmegaM	-	0.2	0.2	0.2
Ca	m/s	489.897948556	alpha1	*	10.5	11	11.5
u	m/s	212.581102892	e	-	0.3	0.3	0.3
xa	-	0.43392935920	BladeHeightDe	mm	2	2	2
TDPoint0.X	kJ/(kg K)	1	dp	mm	502	534.9825	573.81
C0	m/s	0	deltalp	mm	0.25	0.25	0.25
EhC0	kJ/kg	0	zp	-	15	15	15
Ehn	kJ/kg	110.4	DeltaZ	mm	1.5	1.5	1.5
TDPoint1t.S	kJ/(kg K)	6.7535086924	MiuDeltal	-	0.303	0.303	0.303
TDPoint1t.H	kJ/kg	3042.34748636	Miut	-	0.58176	0.58176	0.58176
TDPoint1tX	-	1	TDPoint0.S	kJ/(kg K)	6.8390572473	7.3370721196	7.6731986389
EhnStar	kJ/kg	110.4	TDPoint0.H	kJ/kg	3083.22385810	3034.66658093	3012.4782970
C1t	m/s	469.893604978	TDPoint0.X	-	1	1	1
fai	fai	0.97	Ca	m/s	771.82992322	618.63077263	665.47432453
C1	m/s	455.796796829	u	m/s	183.99260974	196.08132737	210.31234939
TDPoint0star.S	kJ/(kg K)	6.7535086924	C0	m/s	91.8532514803	382.11899205	318.61591194
TDPoint0star.H	kJ/kg	3152.74748636	EhC0	kJ/kg	4.2185099038	73.007462043	50.758049671
TDPoint0star.X	-	1	Ehn	kJ/kg	238.28857215	153.08161314	177.14243064

Figure 30. Sub Module showing stage by stage calculation results

7) Module ‘Section Calculation’

In the ‘Section Calculation’ module a calculation of stage groups (sections) regarding steam flow rate and section power is done at first. Followed by a series of thermal economic index including inner power, electric power, specific steam consumption with and without steam extraction, heat rate and electrical efficiency.

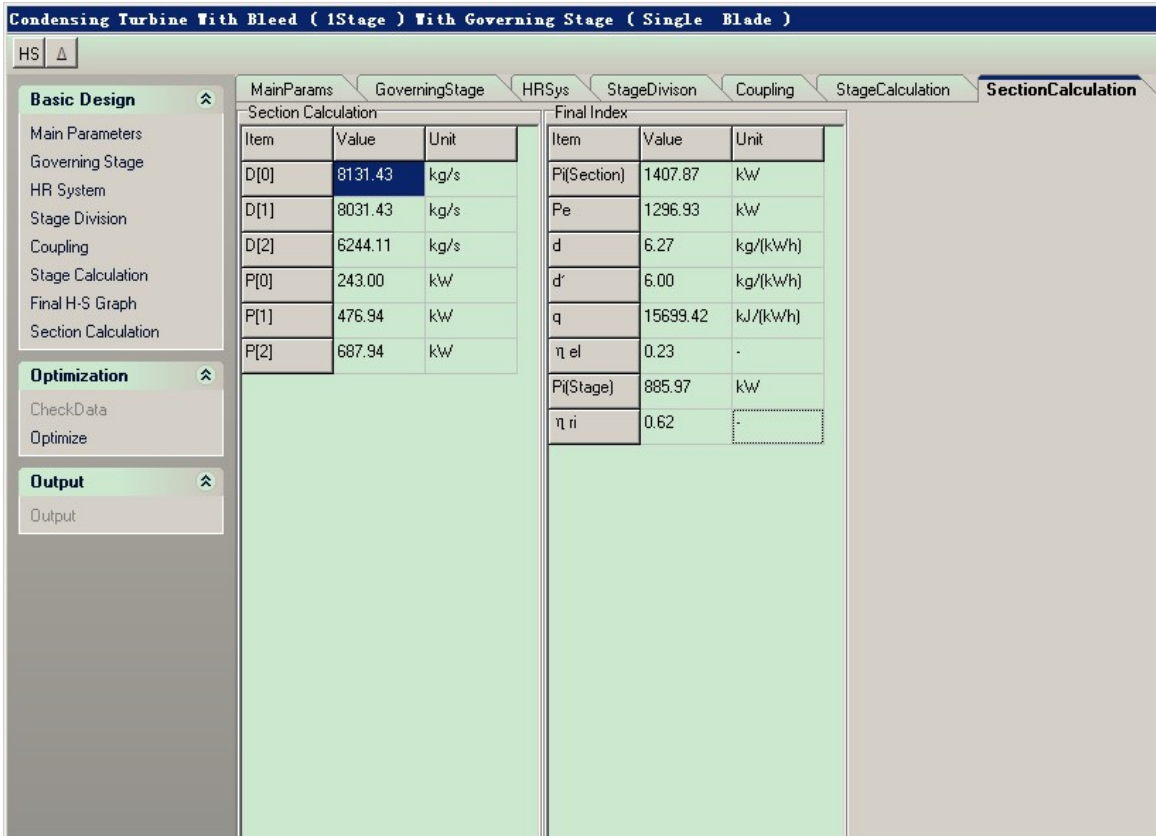


Figure 31. Module 'Section Calculation'

4.3 Data structure

The STFPD is developed based on MVC (Model–view–controller) software architecture pattern^[26] (see Fig.31). The model consists of application data, business rules, logic, and functions. A view acts as a platform for interaction between the data and user. Its main function is to provide GUI (Graphical User Interface). A controller mediates input, converting it to commands for the model or view, providing business logic and constraints. A model is used to encapsulate basic data structures.

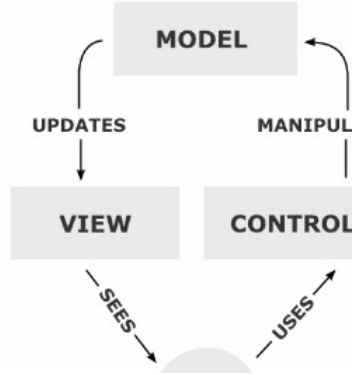


Figure 32. Illustration of the MVC architecture pattern

In STFPD the MVC pattern is reflected in each module. Combining with major features of Delphi as an object-oriented based tool, a unique structure is established in this study.

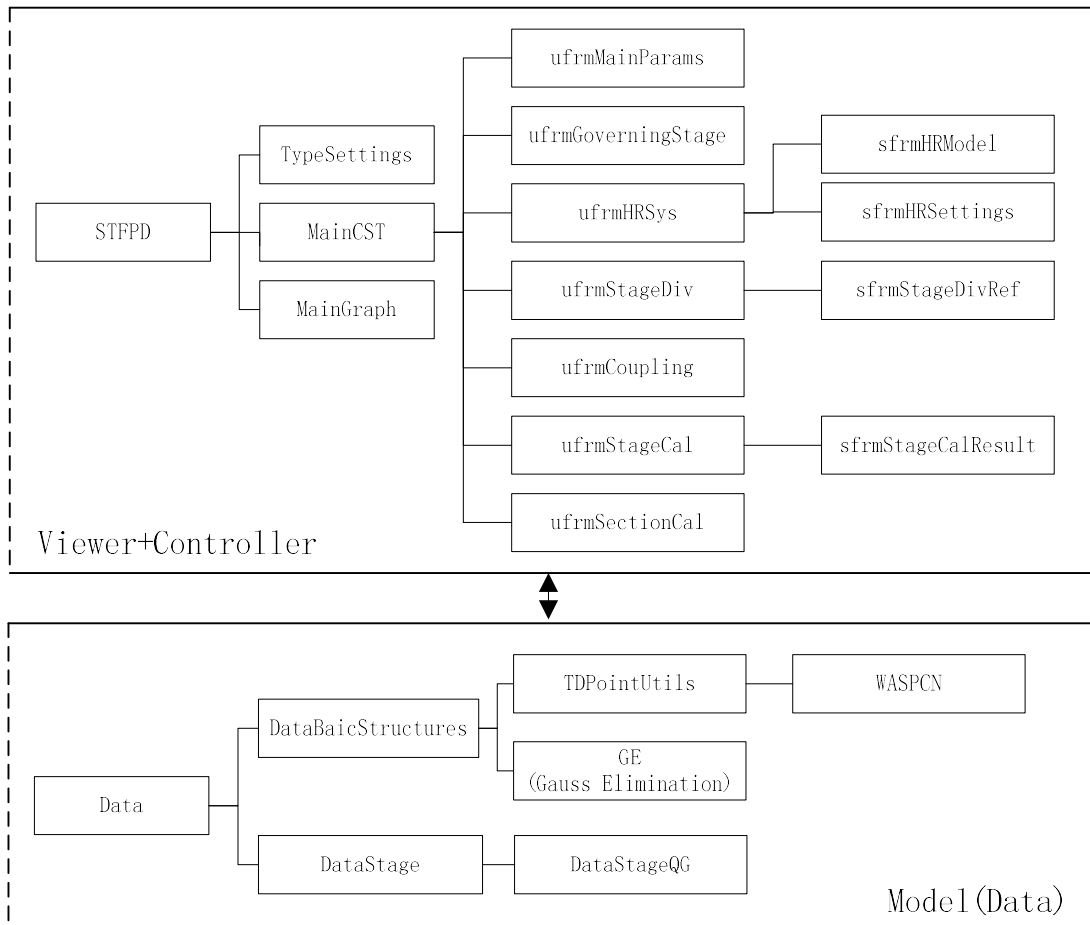


Figure 33. Architecture of STFPD

A list of basic units and their functions is shown in Table 8.

Table 8. List of basic units

Order	Name	Function
1	TypeSettings	Basic type settings of turbine
2	MainCST	Mainframe for STFPD, uses actionlists to control visibility of each frame module.
3	MainGraph	Drawings on a h-s chart
4	ufrmMainParams	Collect initial data and generate approximate thermal dynamic process curve
5	ufrmGoverningStage	Design governing stage
6	ufrmHRSys	Design heat regenerative system
7	ufrmStageDiv	Implement stage division
8	ufrmCoupling	Implement coupling between extraction points and post stage points
9	ufrmStageCal	Stage by stage calculation
10	ufrmSectionCal	Section calculation and generate final index
11	sfrmHRModel	Basic graphic unit of heat regenerative system
12	sfrmHRSettings	Basic table unit of heat regenerative system
13	sfrmStageDivRef	Subroutine, provides a rigid data analysis process based on empirical design, generates dataflow for later use
14	sfrmStageCalResult	Shows detailed design results of each stage
15	Data	Core of STFPD, includes major data structures and algorithm.
16	DataBasicStructures	Includes basic data structures such as records
17	TDPointUtils	All thermal dynamic points related information is processed in this unit
18	WASPCN	External module for thermal dynamic calculations

19	GE	Basic unit for Gauss Elimination algotihm
20	DataStage	Basic unit for a big class TStage
21	DataStageQG	Sub unit of DataStage, providing empirical graph queries

According to Delphi's basic structure, each unit stands for a Class. To utilize this feature, controller logic is planted into each unit class as private statements. As is shown in Fig. 33.

```

Type
TfrmHRSys = class(TFrame)
    RzToolbar1: TRzToolbar;
    Panel1: TPanel;
    PnlHRGrid: TPanel;
    PnlHRIImage: TPanel;
    GroupBox1: TGroupBox;
    RzPanel1: TRzPanel;
    SEditRange: TSpinEdit;
    ActionList1: TActionList;
    actOnChange: TAction;
    SBtnConfirmRange: TSpeedButton;
    actRefresh: TAction;
    BtnRefresh: TButton;
    BtnClearV: TButton;
    BtnDefault: TButton;
    BtnCalculate: TButton;
    BtnDrawCurve: TButton;
    {Events}
    procedure AfterConstruction; override;
    procedure BtnDefaultClick(Sender: TObject);
    procedure BtnClearVClick(Sender: TObject);
    procedure BtnCalculateClick(Sender: TObject);
    procedure      actOnChangeExecute(Sender:
 TObject);
    procedure      BtnDrawCurveClick(Sender:
 TObject);
    procedure      actRefreshExecute(Sender: TObject);
private
    ArrfrmHRModel : array     of
TfrmHRModel;
    ArrfrmHRSettings : array of TfrmHRSettings;

```

```

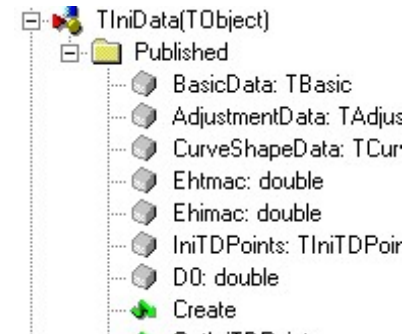
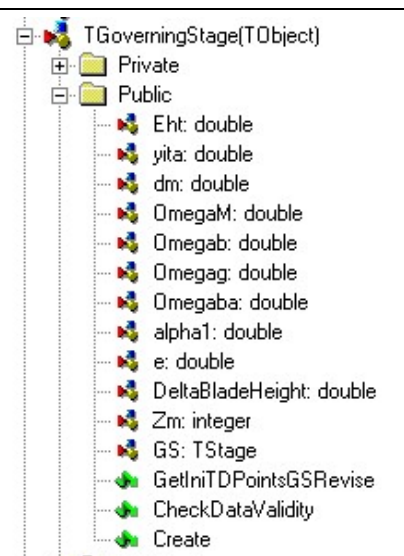
{Visual}
procedure DrawDynGrid(param : TtypeSettings);
procedure CheckV;
{Data}
procedure Ini;
procedure Calculate;
{Data & Visual}
procedure D2V(param: THRSys);
procedure V2D(param: THRSys);
public
end;

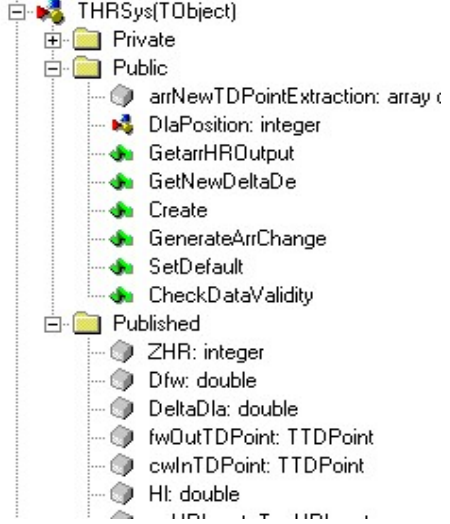
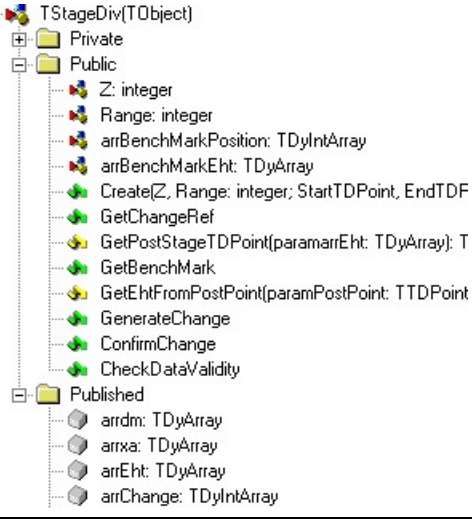
```

Figure 34. Illustration of module structures

Each module contains a class which includes all its components and corresponding events. By implanting private statements which contains an integrate concept of MVC structure pattern (Visual-Data-Data & Visual), controller and viewer logic is established in this module. Table 9 is a clear illustration of structure analysis of STFPD.

Table 9. Structure analysis of STFPD

Title	Function	Structure Analysis						
		Behaviour	MVC		Events			
MainParams	Get initial H-S Curve	Input Calculate Output (visible)	Data	Ini Calculate	AfterConstruction Default ClearV Calculate Draw	 <pre> TIniData(TObject) Published BasicData: TBasic AdjustmentData: TAdjus CurveShapeData: TCur Ehtmac: double Ehmac: double IniTDPoints: TIniTDPoint D0: double Create ... </pre>		
			Visual	DrawStaticGrid				
			Data- Visual	D2V(input)				
				V2D(input)				
				ShowResult(Output)				
				SaveAndSend(Output)				
GoverningStage	Set and get governing stage, revise H-S curve	Input Calculate Output(visible)	Data	Ini Calculate	AfterConstruction Default ClearV Calculate Draw	 <pre> TGoverningStage(TObject) Private Public Eht: double yita: double dm: double OmegaM: double Omegab: double Omegag: double Omegaba: double alpha1: double e: double DeltaBladeHeight: double Zm: integer GS: TStage GetIniTDPointsGSRevise CheckDataValidity Create </pre>		
			Visual	DrawGrid				
			Data- Visual	D2V(input) V2D(Input) FillSBGSValue(Output) FillDBGValue(Output)				

HRSys	Set HR Δ ht Division	Input Calculate Output (invisible)	Data	Ini Calculate	AfterConstruction Default ClearV Calculate	
			Visual	DrawDynGrid		
				D2V(input) V2D(input) SaveAndSend(Output)		
StageDiv	Set stage Δ ht Division	Ini Auto GetResult Input Draw Output	Data	Ini Calculate	AfterConstruction Default ClearV Calculate	
			Visual	DrawDynGrid CheckV LoadFromResult		
				D2V(input) V2D(input)		

	Coupling	Couple post stage points and extraction points	Ini Choose Calculate Draw	Data	Ini		<p>TCoupling(TObject)</p> <ul style="list-style-type: none"> + Private - Public - Methodflag: integer - arrNewStageDivEht: TDyArray - arrNewStageDivOutTDPoint: TTDPoint - arrNewHRSysOutTDPoint: TTDPo - Z: integer - ZHR: integer - Create(HRSys: THRSys; StageDiv: TStageDiv; Z: integer; ZHR: integer; ArrNewStageDivEht: TDyArray; ArrNewStageDivOutTDPoint: TTDPoint; ArrNewHRSysOutTDPoint: TTDPo): TStageCal - CoupleByStageDivSuggestions - CheckOriData - CoupleByStageDiv - CoupleByHRSysSuggestions - CoupleByHRSys - CoupleByBothSuggestions - CoupleByBoth
				Visual			
	StageCal	Stage by stage calculation	Ini Input Calculate Draw	Data	Ini		<p>TStageCal(TObject)</p> <ul style="list-style-type: none"> + Private - Public - ReviseMu1 - GetOptimumE - GetOptimumAlpha1 - GetOptimumOmega1 - Create(typeSettings: TtypeSetting): TStageCal - GetNewTDProcessCurve - GetYitari - GetSumPi - SolutionGenerator - Published - Z: integer - Stages: TList - yitari: double - SumPi: double - arrm: array of integer - arrG: array of double - arrDm: array of double - arrdn: array of double
				Visual	DrawDynGrid		
				Data-Visual	D2V(input) V2D(input)		

4.4 Program Test

Test of the program is based a set of available 25MW condensing steam turbine design data^[21]. The comparison results are shown as follows:

- Governing Stage

Table 10. Comparison between benchmark and STFPD results (Governing Stage)

Stage Inlet parameters	Item		Type:	Dual Row		
	Property	Item	Unit	BenchMark	STFPD	error
	Steam Flow Rate	G	kg/s	23.9	23.9	0%
	Pre-stage pressure	p0'	Mpa	3.305	3.305	0%
	Pre-stage enthalpy	h0'	kJ/kg	3304.2	3304.2	0%
	Pre-stage specific volume	v0'	m3/kg	0.0955	0.0951	0%
	Meanline diameter	dm	mm	1150	1150	0%
	Ideal enthalpy	Δht	kJ/kg	280	280	0%
	Ideal velocity	Ca	m/s	748.3	748.33	0%
	Circular velocity	u	m/s	181	180.64	0%
	Velocity ratio	xa	—	0.24	0.24	0%
	Partial-arc admission degree	e	—	0.359	0.359	0%
Stage Outlet parameters	Property	Item	Unit	BenchMark	STFPD	error
	Exhaust velocity	C2'	m/s	128.1	126	-2%
	Exhaust direction	α2'	°	89.07	88.15	-1%
	Exhaust losses	Δhc2	kJ/kg	8.2	8	-2%
	Circumferential effective	Δhu'	kJ/kg	223.2	224.6	1%
	Enthalpy drop	—	—	—	—	—
	Circumferential efficiency	ηu'	—	0.7972	0.8021	1%
	Circumferential power	Wu'	kw	224.7	224.66	0%
	Circumferential Efficiency	ηu''	—	0.8026	0.8024	0%
	(Check)	—	—	—	—	—
	Check index	Δηu	—	0.00	-0.00	-
	Blade Height losses	Δhl	kJ/kg	13.4	17.71	32%
	Circumferential effective	Δhu	kJ/kg	209.82	206.88	-1%
	enthalpy drop	—	—	—	—	—
	Circumferential efficiency	ηu	—	0.749	0.739	-1%
	Sectorial loss	Δhθ	kJ/kg	0.085	0.1110	31%
	Friction loss	Δhf	kJ/kg	3.288	3.27	-1%
	Partial arc admission loss	Δhe	kJ/kg	14.27	14.35	1%
	Stage effective enthalpy drop	Δhi	kJ/kg	192.2	189.27	-2%
	Stage efficiency	ηi	—	0.686	0.676	-1%
	Stage internal power	Pi	kw	4594	4523.4	-2%

From the tables above it is clear that apart from differences in blade height losses and sectorial losses, the other results are well within permissible errors (3%). The differences in both losses may due to the adoption of different loss models.

● Pressure Stage

Table 11. Comparison between Bench Mark and STFPD results (pressure stage #1)

Property	Item	Unit	Stage 1		
			BenchMark	STFPD	Error
Steam Flow Rate	G	kg/s	46.77943	46.77943	0.00%
Nozzle meanline diameter	dn	mm	1100	1100	0.00%
Rotor meanline diameter	db	mm	1100	1100	0.00%
Prestage pressure	p0	Mpa	8.38	8.38	0.00%
Prestage temperature	t0		534	534.2877	0.05%
Prestage enthalpy	h0	kJ/kg	3479.6	3479.6	0.00%
Circular velocity	u	m/s	173	173	0.00%
Ideal enthalpy drop	Δht	kJ/kg	112.6	112.6	0.00%
Ideal outlet velocity	Ca'	m/s	475	474.538	-0.10%
Velocity ratio	Xa		0.364	0.364565	0.16%
Degree of reaction	Ωm		0.075	0.075	0.00%
Nozzle ideal enthalpy drop	Δhn	kJ/kg	104.25	104.155	-0.09%
Nozzle Stagnation enthalpy drop	Δhn*	kJ/kg	104.25	104.155	-0.09%
Nozzle ideal outlet velocity	C1t	m/s	456.6	456.4099	-0.04%
Nozzle velocity efficiency	φ		0.97	0.97	0.00%
Nozzle outlet velocity	C1	m/s	443	442.7176	-0.06%
Nozzle losses	δhn	kJ/kg	6.2	6.155561	-0.72%
Post nozzle pressure	p1	Mpa	6.13	6.17188	0.68%
Post nozzle temperature	t1		484	483.5627	-0.09%
Post nozzle specific volume	v1	m³/kg	0.0552	0.053587	-2.92%
Nozzle venting area	An	cm²	58.86	56.38564	-4.20%
Sinus of nozzle inlet steam angle	sinα1		0.2236	0.22359	0.00%
Nozzle inlet steam angle	α1	°	12.92	12.92	0.00%
Nozzle Blade Height	ln	mm	22.9	21.92752	-4.25%
Partial-arc admission degree	e		0.3328	0.3328	0.00%
Roter blade inlet steam velocity	w1	m/s	278.5	276.8133	-0.61%
Rotor inlet kinetic energy	Δhw1	kJ/kg	38.73	38.31281	-1.08%
Ideal enthalpy drop in rotor	Δhb	kJ/kg	8.46	8.445	-0.18%
Rotor stagnation enthalpy drop	Δhb*	kJ/kg	47.19	46.75781	-0.92%
Rotor outlet velocity efficency	w2t	m/s	306.8	305.7939	-0.33%
Rotor oulet velocity coefficient	Φ		0.921	0.921	0.00%
Rotor ouelet velocity	w2	m/s	282	281.6362	-0.13%
Rotor blade losses	δhb	kJ/kg	7.16	7.095919	-0.89%
Rotor outlet velocity	C2	m/s	132.7	131.5855	-0.84%
Exhaust losses	δhc2	kJ/kg	8.79	8.657372	-1.51%
Post steage pressure	p2	Mpa	6.01	6.015851	0.10%

Post stage temperature	t2		492	482.1882	-1.99%
Post stage specific volume	v2	m-3	0.0572	0.054935	-3.96%
Rotor venting area	Ab	m2	95.82	91.24645	-4.77%
Sinus of exhaust direction	sinβ2	—	0.3374	0.331583	-1.72%
Exhaust direction	β2	°	19.72	19.36489	-1.80%
Rotor Blade Height	lb	mm	24.7	23.92752	-3.13%
Blade Height losses	δhl	kJ/kg	6.32	4.963141	-21.47%
Circumferential effective enthalpy drop	Δhu	kJ/kg	84.15	85.72801	1.88%
Circumferential efficiency	ηu"		0.7472	0.805406	7.79%
Friction loss	δhf+δhe	kJ/kg	8.04	9.631702	19.80%
Stage effective enthalpy drop	Δhi	kJ/kg	76.12	70.07387	-7.94%
Stage efficiency	ηi		0.6758	0.622326	-7.91%
Stage internal power	Pi	kw	3595.6	3278.016	-8.83%

Comparison between benchmark and STFPD in one of the pressure stages design results implies the same conclusion as before: the results generated by STFPD are generally reliable, apart from differences brought by different loss models.

Chapter 5 Design of turbine system for a 1MW parabolic trough solar thermal power plant using STFPD

In this study, a 1MWe one stage regenerative steam turbine is designed as the center piece of the power block for an under-discussion demonstration solar thermal power plant based on PT technology.

5.1 Case description

The demonstration project Liangzi Lake 1MW parabolic trough solar thermal power plant is located in the Southeast of Wuhan. Its terrestrial coordinates are $30^{\circ}14'56''N$, $114^{\circ}32'32''E$. The annual direct global horizontal irradiation is around $1300\sim1400\text{ kwh/m}^2$. Fig. 35 shows the general scheme of the whole plant.

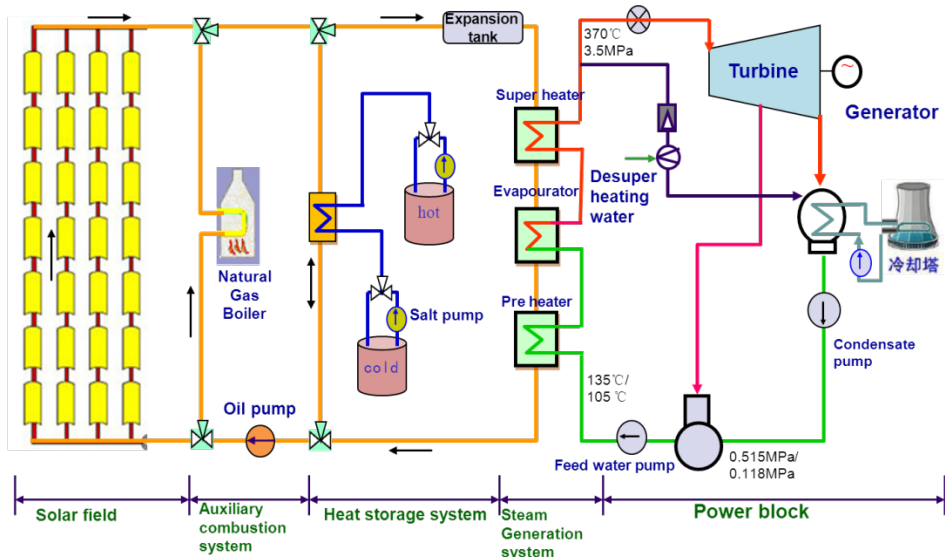


Figure 35. Scheme of Liangzi Lake 1MW parabolic trough solar thermal power plant

General information of a plan for solar field is given as follows.

Table 12. A plan for solar field using ET150 parabolic trough collector

Reflective aperture area	817.5 m^2
Aperture width	5.776 m
Assembly Length	150 m
Module number per assembly	12
Average focal length	2.11 m
Piping distance between assemblies	1 m
Absorber tube inner diameter	0.066 m
Absorber tube outer diameter	0.07 m

Glass envelope inner diameter	0.115 m
Glass envelope outer diameter	0.12 m

The plant uses heat transfer oil as the working fluid in the upstream system of the power block. Due to features of parabolic trough technology, the temperature of heat carrier is expected to be less than 400°C in the solar field. In this case during working hours the temperature of working fluid is estimated to be 390°C, considering a 20°C difference in temperature caused by heat transfer, the objective inlet steam temperature is 370°C.

Under the framework of the plant, considering the power block only, inlet steam of 370°C, 3.5MPa goes into the steam turbine and produce work. According to the size of the cycle, it is advisable to have one extraction point from the steam turbine, hence a deaerator is used to heat the inlet condensate water which is later pumped into the preheater as feed water. Wet cooling is assumed in the condensate system. For that reason, the condensation pressure is extremely low as 0.006 MPa, favorable value to increase the power cycle efficiency. Common parameters for the power block considered are showed in Table 13.

Table 13. Design Point parameters for the 1MWe Rankine power cycle

<i>Turbine</i>	
Isentropic efficiency	~0.64
Electro-mechanical efficiency	0.98
<i>Condenser pump</i>	
Outlet pressure (MPa)	1.2
<i>Feedwater pump</i>	
Outlet pressure (MPa)	6.3
<i>Deaerator</i>	
Pressure (MPa)	0.118/0.515
<i>Condenser</i>	
Pressure (MPa)	0.006

Since the size of the plant is 1MW, considering the plant's own electricity demand, the rated power of the turbine is set at 1.5MW. According to empirical data, the design point for capacity under 6MW is around 75%~90% of the rated power^[21], hence a design point of 1.2 MW is considered.

In heat regenerative system, a deaerator is used provided with two schemes: working pressure of 0.515 and 0.118. The corresponding feed water temperature is 153°C and 105°C respectively.

5.2 Case studies

In this paper, to achieve a relatively high efficiency also consider manufacture costs, various cases were tried and compared. Three cases in particular were picked out to represent features of a solar thermal steam turbine. Among these demonstrated cases, case 1 and case 2's difference lies in different choices for stage numbers, case 2 and case 3's comparison represents the difference in design results considering different heat regenerative system schemes.

Table 14. Case comparisons

Property	Item	Unit	Case 1	Case 2	Case 3
Inlet steam mass flow rate	D0	Kg/h	9593.15	9044.82	8680.46
Rotational speed	n	r/min	5400	5400	5400
Inlet pressure	p0	MPa	3.5	3.5	3.5
Inlet temperature	t0	°C	370	370	370
Exhaust pressure	pc	MPa	0.006	0.006	0.006
Stage division			1g+5p	1g+8p	1g+8p
Extraction point position (post pressure stage)			1	1	4
Deaerator pressure	pe _{DA}	MPa	0.515	0.515	0.118
Bleed temperature	t _{bleed}	°C	265.8	296.3	156.5
Bleed mass flow rate	Δ De	Kg/h	1592.5	1467.995	911.103
Feedwater temperature	t _{feedwater}	°C	153	153	105
Governing stage nozzle meanline diameter	dn(governing stage)	mm	590	560	560
Governing stage rotor meanline diameter	dm(governing stage)	mm	590	560	560
Governing stage arc-partial admission degree	e	-	0.15	0.15	0.15
Governing stage nozzle blade height	ln(governing stage)	mm	11.7	11.5	11
Governing stage rotor blade height	lb(governing stage)	mm	13.7	13.5	13
Governing stage guiding blade height	lg(governing stage)	mm	15.7	15.5	15
Governing stage second rotor blade height	lb'(governing stage)	mm	17.7	17.5	17
First pressure stage nozzle meanline diameter	dn(1st pressure stage)	mm	560	520	520
First pressure stage rotor meanline diameter	db(1st pressure stage)	mm	560	520	520
First pressure stage nozzle blade height	ln(1st pressure stage)	mm	15.7	11.9	11.4
First pressure stage rotor blade height	lb(1st pressure stage)	mm	17.7	13.9	13.4
Last pressure stage nozzle meanline diameter	dn(last pressure stage)	mm	677	591	591
Last pressure stage rotor meanline diameter	db(last pressure stage)	mm	678	591	591
Last pressure stage nozzle blade height	ln(last pressure stage)	mm	81.1	98.8	100.2
Last pressure stage rotor blade height	lb(last pressure stage)	mm	83.1	100.8	102.2
Governing stage enthalpy drop	Δ ht(governing stage)	KJ/kg	105.3	104.2	103.9
Pressure stage enthalpy drop	Δ ht(pressure stages)	KJ/kg	562.2	633.1	622.9
Turbine internal power	Pi	kW	1384.5	1414.3	1465.9
Shaft end power	Pa	kW	1282.6	1282.9	1329.7
Generator power output	Pe	kW	1205.6	1193.1	1236.6
Turbine relative internal efficiency	η _{ri}	-	62.1%	68.6%	67.6%
Turbine efficiency	η _i	-	22.8%	23.4%	23.7%

As can be seen from the comparison between case 1 and case 2, a reduction in number of stages brings about a slight increase in turbine mean line diameter (in other words, the turbine size). This is reasonable since $\Delta h_t = \frac{\pi^2 d_m^2 n^2}{2000 \times 60^2 \times x_a^2}$, fewer stages means higher enthalpy drop for each stage, with constraints of maintaining the same rotational speed and velocity ratio, mean line diameter has to increase. Due to changes in enthalpy drop distribution, post stage points hence extraction points changes. As a result a slight increase in bleed mass flow rate can be seen in case 1. Due to larger ideal enthalpy drop, since $C_{lt} = 44.72\sqrt{(1-\Omega_m)\Delta h_t}$ velocity increases dramatically and brings about more fluid dynamic losses. From another version of description, larger enthalpy drop means larger pressure ratio which may lead to supersonic flow, if it goes out of a certain range other losses would come about. Hence theoretically fewer stage number schemes usually result in less efficiency. The idea is proved by efficiency indexes in case 1 and case 2, where the six stages scheme shows lower efficiency than the nine stages scheme ($\eta_{ri} = 62.1\%$ in case 1 compared to 68.6% in case 2, $\eta_i = 22.8\%$ in case 1 compared to 23.4% in case 2).

According to comparison between case 2 and case 3, choice of deaerator has a certain impact on turbine efficiency, with the former case showing 68.6% in turbine internal efficiency compared to 67.6% in the latter case. Other differences include inlet steam mass flow rate and extraction steam mass flow rate, obviously high pressure scheme costs more steam than the low pressure scheme, with 9044 kg/h compared to 8680 kg/h . Regarding impact of extraction steam on pressure stages, in case 2 (high pressure extraction scheme) extraction point is located at the end of the first pressure stage, moisture losses happens at the sixth stage with a degree of dryness of 0.950 at the last stage, whereas in case 3 (the low pressure extraction scheme) extraction point is located at the end of the fourth pressure stage, moisture losses happens at the seventh stage with a degree of dryness of 0.954 at the last stage. Since a constraint of rotational speed and stage number is given, the size of turbine doesn't have much difference.

5.3 Conclusions

According to case studies results, compared to normal steam turbines, features of steam turbines for parabolic trough solar thermal technology include:

- High rotational speed;
- Small in size (with mean line diameter of around $500\text{--}600 \text{ mm}$);
- Relatively smaller velocity ratio;
- Small nozzle outlet angle;
- Most stages have to endow partial admission to avoid small blade heights.
- If number of stages is limited due to manufacturing cost considerations, fewer

stages schemes may result in supersonic flow and thus requires special treatment with shapes of nozzle and rotor blade.

- Relatively lower turbine efficiency due to low inlet temperature and smaller size.
- Relatively lower degree of dryness in the last stage. To avoid this phenomenon, reheat system can be added to the cycle.

Usually the more stages, the higher efficiency of the turbine, yet more stages means more manufacture costs, also the number of stages should not be too small, since fewer stages may bring about supersonic flow, which requires extra cost to adopt supersonic nozzles, hence a balance between stage number and stage efficiency should be considered. With regard to adoption of heat regenerative system, two schemes were carried out and compared in this study. Results show that different extraction schemes have a slight impact on turbine efficiency, and they are directly related to the position of extraction points.

Chapter 6 Conclusions and future work

6.1 Research conclusions

Electricity generation from solar thermal energy can be a useful alternative concerning fossil fuel conservation as well as CO₂ emission reduction. However, among various researches regarding this field, the focus had hardly been the solar thermal specialized steam turbine. Due to commercial reasons most power stations would rather buy a turbine from the market than doing researches on it. In this thesis, a basic design platform has been developed for a megawatt level steam turbine in Borland Delphi. The main achievements of the project are:

- 1) A typical process of one dimensional steam turbine flow path design was studied first, then an optimized design method was brought up. The ideal is to add a new standard design phase named ‘Coupling’ before stage by stage calculation. Among three types of coupling, the most complicated one integrates with an optimum-solution-finding algorithm, which helps in rapidly determining the best solution.
- 2) The new turbine design process was realized in Borland Delphi based on object oriented programming paradigm and MVC software architecture pattern, forming a practical and user friendly design software named ‘STFPD (Steam Turbine Flow Path Design)’. The results were compared with design data from an existing 25MW condensing steam turbine, comparisons show that except for two differences which lie in the mathematical models of stage losses, the rest results were generally reliable from STFPD.
- 3) Finally using STFPD, several cases were studied and compared regarding the design schemes of power block for 1MW Liangzi Lake parabolic trough solar thermal power plant, a conclusion of features for megawatt level solar thermal specialized steam turbines was drawn.

6.2 Future work and suggestions

Future work may include the following aspects:

- 1) Adoption of other forms of optimization.

Regarding one dimensional design itself, more advanced optimization method can be adopted and added into the STFPD as individual modules.

- 2) Varying conditions calculation.

STFPD presently only provides basic functions for design-point design. Off-design point calculations can be added into it as extra modules in order to check design results.

3) 2D and 3D design.

One dimensional design is only the first phase of a modern design procedure. It gives a broad view of potential features of a steam turbine. Under the guideline of preliminary design, further design adopting more complicated fluid mechanical theories has to be carried out. Then the final results can be checked by numerical methods.

4) Add heat regeneration module.

Considering different user demands, an extra module of heat regeneration system can be added into STFPD.

5) Reform software with Database.

STFPD can be upgraded into higher versions considering adoption of database.

Acknowledgements

First I would like to express my heartfelt gratitude to Professor Wang Kun for his constant and illuminating guidance. Without his patience and encouragement, I would not be able to overcome the fear and even find the pleasure in coding. I have benefited enormously from discussing and working with him and I am really thankful for what he has given me.

My deepest gratitude goes to Professor Huang Shuhong who plays such a father like role in caring for every student of his, I consider him a role model in every aspect of life. I'm extremely grateful for his constant inspiring, understanding and guiding. His guidance and advices have been and will always be the light house for the voyage of my life.

My big thanks goes to professor Quentin Falcoz, for his kindness, patience and always-in-time guidance. Also I need to thank prof. Zhang Yanping, prof.Lu Luyi for their kind help during the past two years.

I would like to express my thanks to all the Chinese and European teachers and staff of Institute of Clean and Renewables Energy (ICARE). Special thanks to Ms. Liu Yang for her kind help in recent two years. ICARE provides me with a great platform to develop my skills in both studies and communications (It is really an unforgettable experience studying in ICARE, I've meet so many brilliant people both from China and EU, together we've created so many wonderful memories). I should say I really love this program and I hope it only gets better in the future.

Also I won't forget the encouragement and helps from my dear fellow friends. Young and beautiful, they always bring bright colors to my life. Great thanks to Doctor Zhang Pingting and Doctor Long Rui for being so kind to give precious suggestions on revising this paper. Special thanks to Reuben Harding for his constant supporting during the whole summer. I am blessed to meet this really good friend with such pureness and kindness.

Last but not least, I want to dedicate my thanks to my beloved parents and families. They are the source of my strength — it is with their love and support that I have the courage to fight for my dreams.

References

- [1] NREL: //www.nrel.gov/csp/solarpaces/parabolic_trough.cfm
- [2] Wikipedia
- [3] Niknia I, Yaghoubi M. Transient simulation for developing a combined solar thermal power plant. *Appl Therm Eng* 2012;37:196e200.
- [4] Montes MJ, Abanades A, Martínez-Val JM. Performance of a direct steam generation solar thermal power plant for electricity production as a function of the solar multiple. *Solar Energy* 2009;83:679e89.
- [5] Zarza E, Rojas ME, González L, Caballero JM, Rueda F. INDITEP: the first precommercial DSG solar power plant. *Sol Energy* 2006;80:1270e6
- [6] Wang M, Wang J, Zhao Y, Zhao P, Dai Y. Thermodynamic analysis and optimization of a solar-driven regenerative organic Rankine cycle (ORC) based on flat-plate solar collectors. *Appl Therm Eng* 2013;50:816e25
- [7] Al-Sulaiman, F. A. (2013). "Energy and sizing analyses of parabolic trough solar collector integrated with steam and binary vapor cycles." *Energy* 58(0): 561-570.
- [8] Shuhong, H., Fundamentals of Steam Turbine. 2008: CHINA ELECTRIC POWER PRESS.
- [9] Jun, W., Three Dimensional Design Fundamentals of Fluid Machinery. 2008: Wuhan.
- [10] Naining, W., ed. Thermal Dynamic Design of Steam Turbine. 1987, China WaterPower Press.
- [11] Chen Lingen, Zhang Junmai. Present status of axial turbine flow path optimization design. *Power Engineering*, 1989(04): 10-13+62.
- [12] Chen Lingen, Progress in turbo machine optimization design in recent decades. *Thermal energy and power engineering*, 1992(04): 214-221.
- [13] Chen Lingen, Optimization design of stage groups in a multistage steam turbine. *Power System Engineering*, 1996(03): 9-13+63.
- [14] Xin Zhe, Zou Zixiang, Geometric optimizaiton design of turbo machinery. *Journal of China Agricultural University*, 1998(06): 75-79.
- [15] Qin Xiaoyong, Chen Lingen etc. Optimizaiton for a steam turbine stage efficiency using a genetic algorithm. *Applied Thermal Engineering* 23(2003): 2307-2316.
- [16] Axstream user manual vol.3
- [17] <http://www.energy.siemens.com.cn/Energy/OilandGas/IP/IndustrialSteamTurbines/Predesignedsteamturbines/Documents/Pre-designed%20Steam%20Turbines%20en.pdf>
- [18] <http://www.energy.siemens.com.cn/Energy/OilandGas/IP/IndustrialSteamTurbines/SST100/Pages/Default.aspx#Technical%20data>
- [19] Zarza, E., M. E. Rojas, et al. (2006). "INDITEP: The first pre-commercial DSG solar power plant." *Solar Energy* 80(10): 1270-1276.
- [20] Leonid Moroz, Yuri Govorushchenko, Petr Pagur. A UNIFORM APPROACH TO

CONCEPTUAL DESIGN OF AXIAL TURBINE/COMPRESSOR FLOW PATH.
The Future of Gas Turbine Technology 3rd International Conference 11-12
October 2006, Brussels, Belgium.

- [21]Xiao Zenghong, W.L.E., ed. Steam Turbine Course Design. 2012, CHINA ELECTRIC POWER PRESS: Beijing.
- [22]LI Wei. R&D on a software for thermodynamic designing of industrial steam turbines [D]. Zhe Jiang University, 2007.
- [23]Feng Huiwen. Instructions for steam turbine course design, 1992.
- [24][JBR99] Ivar Jacobson, Grady Booch, James Rumbaugh: The Unified Software Development Process; Addison Wesley, ISBN 0-201-57169-2, 1999
- [25]Paul F. McCombie, Jim Penman. The production of interactive engineering design software using Borland Delphi; Advances in Engineering Software, Volume 32, Issues 10–11, October–November 2001, Pages 789-796.
- [26]Simple Example of MVC (Model View Controller) Design Pattern for Abstraction. <http://ist.berkeley.edu/as-ag/pub/pdf/mvc-seminar.pdf>.